

Using a GIS-based order weight Average (OWA) Methods to Predict Suitable Location for Artificial Recharge of Groundwater

Marzieh Mokarram (✉ m.mokarram@shirazu.ac.ir)

Shiraz University <https://orcid.org/0000-0003-4282-1950>

Saeed Negahban

Shiraz University

Ali Abdolali

University Corporation for Atmospheric Research

Mohammad Mehdi Ghasemi

Shiraz University

Research Article

Keywords: Artificial recharge of groundwater (ARG), fuzzy -AHP method, Ordered Weight Average (OWA)-AHP, ANFIS, Best subset

Posted Date: February 24th, 2021

DOI: <https://doi.org/10.21203/rs.3.rs-178899/v1>

License:   This work is licensed under a Creative Commons Attribution 4.0 International License.

[Read Full License](#)

41

42 **1. Introduction**

43 Water scarcity is a major concern in different parts of the world, especially in semi-arid and arid
44 areas. The lives of about one-third of the world's population are tied to groundwater and more than
45 70% of groundwater resources are consumed by agriculture (FAO, 2017). The withdrawal of these
46 resources is increasing due to the rapid agricultural and industrial growth. Consequently, excessive
47 groundwater consumption causes irreversible problems such as a significant drop in the water level
48 of wells and drying, river flow reduction, lake level subsidence, water quality degradation, and an
49 increase in pumping costs. The artificial recharge of groundwater (ARG) is among the most
50 efficient ways for control and prevention of water level decrease in plains, which is of great
51 importance for agriculture and industry. Artificial recharge is a series of pre-designed activities for
52 the nourishment of groundwater either by natural replenishment or percolation of surface waters
53 into the groundwater aquifers, leading to increase in groundwater volume (National Research
54 Council, 1994). Thus, locating suitable areas for artificial recharge is important.

55 Geographical Information System (GIS) is a tool for data analysis that can be used to store,
56 retrieve, manipulate, process and analyze different spatial and temporal datasets (Palanisamy et al.
57 2020). This tool provides accurate spatial information about the watershed for conservation and
58 planning in water resources management (Karunanidhi et al. 2019). There are different ways to
59 determine the appropriateness of a region for artificial recharge in GIS. Rajasekhar et al. (2019)
60 used Remote Sensing (RS), GIS, and Analytical Hierarchy Process (AHP) technique to predict
61 Artificial Groundwater Recharge in Anantapur District, India. The results showed that the
62 accuracy of methods to determine a suitable location was 82.05%.

63 Kim et al. (2018) used the Artificial Neural Network (ANN) method to determine the situation of

64 groundwater recharge in South Korea. The results showed that if the ANN model score is less than
65 1.5, the possibility of artificial recharging is relatively low. Patil et al. (2019) used GIS and Remote
66 Sensing (RS) techniques to determine suitable locations for groundwater recharge. The results
67 showed high accuracy in classifying the area into good, medium, and poor classes for groundwater
68 recharge. Anand et al. (2020) used the AHP method in GIS to determine suitable locations for
69 groundwater recharge in the Bhavani River basin of South India. The results showed that the best
70 areas for groundwater recharge are dams. Arya et al. Arya et al. (2020) used the AHP method to
71 determine suitable locations for groundwater recharge in the Vattamalaikarai River basin in South
72 India. They found that more than 50% of the area was in the medium or low potential group in
73 terms of groundwater.

74 Das et al. (2019) used fuzzy-AHP to determine land suitability for groundwater recharge in West
75 Bengal, India. According to their results, the plain in the east of the area was suitable for
76 groundwater recharge. Rajasekhar et al. (2019) used the AHP method to determine artificial
77 groundwater recharge in the Jilledubanderu river basin. They concluded that fuzzy-AHP is an
78 accurate method for predicting land suitability for artificial groundwater recharge. Kamangar et al.
79 (2020) used AH, ANP, and TOPSIS to weigh the effective parameters of ARG in southern Iran.
80 The results showed that about 5% of the study area was suitable for artificial recharge of
81 groundwater. Arya et al. (2020) used GIS and RS to prepare interpolation maps of groundwater
82 potential. Their results indicated that more than 50% of the basin region falls under the moderate
83 to low groundwater potential category.

84 One of the methods that have been used for land suitability in some recent studies is the Order
85 Weight Average (OWA) method which, unlike other multiple-criteria decision analysis (MCDA)
86 methods such as AHP and ANP, is able to prepare land suitability maps with different levels of

87 risk that, depending on the environmental and regional conditions, can be used by managers for
88 ARG. OWA is widely used in multi-criteria combination procedures (Bellmann , 1970;
89 Malczewski et al., 2003; Malczewski, 2006; Mokarram and Aminzadeh, 2010). It provides a
90 different decision strategy with various risks (Malczewski and Rinner, 2005; Chu and Lin, 2009;
91 Ban and Ban; 2012).

92 According to studies and the importance of ARG in arid and semi-arid regions, it is important to
93 check and determine suitable places for groundwater recharge. Considering that the uncontrolled
94 abstraction of groundwater in most arid and semi-arid regions, especially in Iran, has caused a
95 sharp drop in the water table and reduced aquifer reserves, determining suitable locations for ARG
96 is of great importance (Ghayoumian et al., 2007). Annual extraction of 520 million cubic meters
97 of groundwater out of aquifers in Bushehr province in southern Iran has reduced these aquifers.
98 Therefore, groundwater resource management and ARG in the study area is important. The
99 purpose of this research is to determine the location of artificial recharge in southern Iran, taking
100 into account the geographical and atmospheric parameters such as slope, lithology, land use,
101 drainage density, distance to fault, precipitation, and altitude. In this study, a new hybrid method
102 called OWA-AHP is used which advantageously provides us with the combination of two-by-two
103 comparisons of each parameter using the AHP method and use of different risk levels using the
104 OWA method. This makes the OWA method more efficient for weighting layers. In this study,
105 using the ANFIS method, land suitability classes for ARG are also predicted through input
106 parameters. Finally, using the best subset regression method, the most important parameters
107 affecting ARG are identified. In general, the objectives of the research are as following:

108 1- Using membership functions, the fuzzy maps for each parameter are prepared and using the
109 AHP method, the weight of each parameter is determined and the final map of suitable places for

110 ARG is prepared.
111 2- A combination of OWA-AHP is used as a new efficient tool to weigh each layer and prepare
112 land suitability maps with different levels of risk.
113 3- The ANFIS method is used to predict land suitability classes.
114 4- The best subset regression method is used to determine the most important parameters
115 affecting groundwater recharge.

116

117 **2. Materials and methods**

118 In this part, the membership functions are defined by the fuzzy maps for each parameter and
119 prepared. Then AHP method is used to compare the importance of each parameter in a pairwise
120 comparison to determine the weight of each parameter. Using the OWA-AHP method, suitability
121 maps with different levels of risk are prepared. ANFIS is used to predict land suitability classes
122 and the best subset regression method is used to determine the most important effective parameters
123 in suitable places for ARG. A summary of the research method is shown in Fig. 1.

124

125 *2.1. Study area*

126 This study was carried out in Bushehr Province, located in the south of Iran. It has an area of
127 42,871.23 km² with a population of 1,163,400 and lies between the longitude of 27 ° 01 ' to 29 °
128 54 ' N and latitude of 51 ° 12 ' to 55 ° 42 ' E (Fig. 2). The province connects to the Persian Gulf on
129 its south. The temperature values in the region range between -1 and 52.5 C° and the average
130 annual temperature in the province is 25.7 C°. The vegetation of the study area varies and depends
131 on the geographical location of the area so that, in warm and dry areas, most of the native species
132 are Acacia. Two permanent rivers including Mand (685 km), and the Hell River (230 km) flow in

133 the study area (Pazira et al., 2016).

134

135 *2.2. Preparing raster maps*

136 In this study, slope, lithology, land use, drainage density, distance to fault, precipitation, and
137 altitude maps are used as input data to determine the suitable locations for ARG. The description
138 of factors used in the analysis of this stage of the research is listed in Table 1.

139 It is worth noting that the selection of the most important data for the intended purpose depends
140 on the region and expert opinion. For example, Rajasekhar et al. (2019) used geology,
141 geomorphology, drainage density (DD), land use/land cover (LULC), lineament density (LD),
142 slope, soils, and rainfall, or Anand et al. (2020) used drainage, lineament, geology, soil, slope,
143 geomorphology, and land use as input data to determine suitable locations for groundwater
144 recharge. To select the data in the present research, the characteristics of the region and the opinion
145 of experts are used.

146 Finally, interpolation maps are prepared for each parameter with a resolution of 30 m in GIS (Fig.
147 3). In Fig. 3, it can be seen that the southern half of the study area has lower heights and slopes
148 than the northern half. Also, Fig. 3 clearly shows that, except for a small part of the south of the
149 region, the rest of the region has less distance from the faults. The land-use status of the study area
150 is shown in Fig. 3, which shows that the southern parts mostly include rangelands. Also, the
151 susceptibility map of formations to water erosion showed that the southern half is very sensitive
152 to water erosion. The sensitive classes of formation to water erosion are shown in Table 2. Also
153 according to Fig. 3, it turned out that the northern parts have precipitation of more than 400 mm.
154 The drainage density interpolation map is shown in Fig. 3. It is obvious that the northern parts
155 have a higher drainage density.

156

157 2.3.Methods

158 2.3.1. Fuzzy method

159 To prepare fuzzy maps for each parameter, membership functions are used. A fuzzy set A in a
160 reference set X is shown in Eq. (1) (McBratney and Odeh, 1997).

161
$$A = \{x, \mu_{A(x)} \mid x \in X\} \tag{1}$$

162 where $\mu_A(x)$ is called the membership function (or MF) of x in A .

163 In this study, two incremental and decremental membership functions are used to prepare a fuzzy
164 map for each of the parameters, which is shown in Fig. 4. For altitude, precipitation, and drainage
165 density parameters incremental membership function is while for the other parameters decremental
166 membership function.

167

168 2.3.2. Analytic hierarchy process (AHP)

169 The analytic hierarchy process (AHP) is one of the most efficient methods of multi-criteria
170 decision making (Saaty and Vargas,1980). This method is based on a pairwise comparison of
171 parameters and allows managers to examine different scenarios. This method is one of the most
172 comprehensive systems designed for criteria decision making and allows the problem to be
173 formulated hierarchically. It is also possible to consider different quantitative and qualitative
174 criteria in the problem together. This method includes the following steps:

175 A) Creating a hierarchical structure

176 B) Preference of parameters

177 C) Preparation of normalized matrix and weight vector of parameters:

178 To calculate the weight of each parameter, the values of each column of the pairwise comparison
179 matrix must first be added together and each element in the matrix must be divided by the sum of

180 its own column (Eq. 2) Then the average of the elements in each row of the normalized matrix is
 181 calculated (Eqs. 2, 3).

$$182 \quad r_{ij} = \frac{a_{ij}}{\sum_{i=1}^m a_{ij}} \quad (2)$$

$$183 \quad W_i = \frac{\sum_{i=1}^n r_{ij}}{n} \quad (3)$$

184 Here, m is the number of columns, n is the number of rows, a_{ij} is the pairwise comparison matrix,
 185 r_{ij} is the normalized matrix assets for options i , and w_i is the weight of option i .

186

187 D) Determining the final score of options (Eq. 4).

$$188 \quad V_H = \sum_{k=1}^n W_k (g_{ij}) \quad (4)$$

189 V_H is the final score of j , W_k is the weight of each criterion and g_{ij} is the weight of the options in
 190 relation to the criteria.

191 E) Calculating the compatibility rate

192 To calculate the compatibility rate, the pairwise comparison matrix (A) must first be multiplied by
 193 the weight vector (W) to obtain a good estimate of $\lambda_{max}.W$ so that $AxW = \lambda_{max}.W$. By dividing
 194 $\lambda_{max}.W$ by W , the value of λ_{max} is calculated. Then the value of the incompatibility index (I.I.) is
 195 calculated using Eq. 5 and the compatibility rate (I.R.) is calculated using Eq. 6 is calculated. If
 196 the incompatibility value is less than 0.1, the compatibility of the decision matrix is acceptable and
 197 if it is more than 0.1, it should be reconsidered.

198
$$I.I = \frac{\lambda_{\max} - n}{n - 1} \quad (5)$$

199
$$I.R. = \frac{I.I}{I.I.R.} \quad (6)$$

200 *2.3.3. Ordered Weight Average (OWA)-AHP method*

201 The two methods of OWA and AHP are not implemented at the same level. AHP is a general tool
 202 for creating a hierarchical model of spatial decision issues, overall process processing, and
 203 evaluation of each process. The evaluation process in AHP uses a simple weighted linear
 204 combination to calculate the values of each raster cell. OWA operator also provides a general
 205 framework for performing processes such as AHP. The nature and structure of these two
 206 algorithms are such that their combination can be used to create a more powerful spatial decision
 207 tool (Yager and Coleman, 1999). To achieve this framework, it is assumed that two steps of AHP,
 208 namely the formation of the hierarchical structure and the calculation of the relative weights of the
 209 criteria, are met by performing a pairwise comparison of the criteria. From this point on, the
 210 problem is processed by OWA-guided quantifiers (Malczewski, 2006). OWA method can
 211 calculate the level of risk-taking and risk aversion of individuals and enter it in the selection of the
 212 final option. OWA operator, F , with dimension n , is an $\mathbb{R}^n \rightarrow \mathbb{R}$ mapping with weight vector $w=(w_1,$
 213 $\dots, w_n)^T$ for an input set of data $X=(x_1, \dots, x_n)$ that are grouped together as (Eq. 7):

214
$$F(x_1, \dots, x_n) = \sum_{i=1}^n w_i b_i = W^T B \quad (7)$$

215 Which applies to the following conditions (Eq. 8):

216
$$W_i \in [0,1] \quad i = 1, 2, \dots, n$$

$$\sum_{i=1}^n w_i = 1 \quad (8)$$

217

218 Where b_i and i are the largest values of the set ascending to descending. The concept of grading is
219 defined as follows: (Eq. 9).

$$1 \leq \alpha \leq \infty$$

$$\sum_{i=1}^n (n-i)$$

$$Orness(w) = \alpha = \frac{1}{n-2} \tag{9}$$

221 Here, OR-ness is between 0 and 1, which indicates the degree of emphasis of the decision-maker
 222 on the better or worse values of a set of indicators or the same risk-taking and risk aversion of the
 223 decision-maker. The degree of Orness or risk-taking indicates the position of OWA operator
 224 between AND (minimum (and OR (maximum)) relationships. A higher degree value (closer to
 225 one) indicates a more optimistic or risk-taking decision-maker, and a lower degree value (the closer
 226 it is to zero) indicates higher pessimism or risk aversion on the part of the decision-maker. In
 227 general, an OWA operator with OR-ness more than 0.5 represents a risk-averse or optimistic
 228 decision-maker; OR-ness = 1 represents a neutral decision-maker; and OR-ness < 0.5 represents a
 229 risk-averse or pessimistic decision-maker. The most important issue in using the OWA operator is
 230 determining its weights. In this paper, the minimum and maximum distance methods are used to
 231 determine the weights of the OWA operator. This model was introduced by Wang and Parkan
 232 (2005) (Eq. 10).

$$Maximum \quad \partial$$

$$\sum_{i=1}^n w_i = 1$$

$$w_i - w_{i+1} - \partial \leq 0 \quad i = 1, \dots, n-1$$

$$w_i - w_{i+1} + \partial \geq 0 \quad i = 1, \dots, n-1$$

$$w_i \geq 0 \quad i = 1, \dots, n$$

$$\tag{10}$$

234 This model is a linear model that determines the weights based on the given grading. In this model,
 235 the distance between adjacent weights under the given calibration is reduced as much as possible.
 236 The weights obtained from this model are regularly distributed and follow an arithmetic
 237 progression.

238

239 *2.3.4. Adaptive neuro-fuzzy inference system*

240 This model, developed by Young in 1996, allows fuzzy systems to use the adaptive backward error
 241 propagation training algorithm in parameter training discussions (Kim, 1998). An ANFIS structure
 242 consisting of a set of fuzzy IF-THEN rules of the TSK type (for one rule only) can be used for
 243 modeling and mapping input-output data. In general, the steps of this network are as follows:

244

245 **Layer 1**, input Nodes: Each node in this layer generates membership values that belong to each
 246 of the appropriate fuzzy sets using the membership function (Eqs. 11, 12).

$$247 \quad O_{1,i} = \mu_{A_i}(x) \quad \text{for } i = 1, 2 \quad (11)$$

$$248 \quad O_{1,i} = \mu_{B_{i-2}}(x) \quad \text{for } i = 3, 4 \quad (12)$$

249 where y and x are non-fuzzy inputs to nodes i , and A_i and B_i are language tags that are denoted
 250 by the membership functions of μ_{A_i} and μ_{B_i} , respectively.

251

252 **Second layer**, rule nodes: Each neuron in this layer is fixed. The "and" operator is used in this
 253 layer until the output that represents the first part of that law is obtained (Eq. 13).

$$254 \quad O_{2,i} = w_i = \mu_{A_i}(x) \mu_{B_i}(y) \quad \text{for } i = 1, 2 \quad (13)$$

255

256 **Third layer**, intermediate nodes: The main purpose of the third layer is to determine the ratio of

257 each ignition power of the law to the sum of all ignition laws. As a result, W is obtained as the
 258 standardized average (Eq. 14).

$$259 \quad O_{3,i} = \bar{w}_i = \frac{w_i}{w_1 + w_2} \quad (14)$$

260 **Fourth layer**, result nodes: In this output layer, each node is equal to (Eq. 15):

$$261 \quad O_{4,i} = \bar{w}_i f_i = \bar{w}_i (p_i x + q_i y + r_i) \quad (15)$$

262 where w_i is the output of the n^{th} node of the previous layer and $\{p_i, q_i, r_i\}$ are the coefficients of
 263 this linear combination

264

265 **Fifth layer**, output nodes: This layer calculates the total single output node by summing all the
 266 input signals. Therefore, in this layer of the non-fuzzy process, the results of each fuzzy law are
 267 transformed into non-fuzzy output (Eq. 16).

$$268 \quad O_{5,i} = \sum_i \bar{w}_i f_i = \frac{\sum_i w_i f_i}{\sum_i w_i} \quad (16)$$

269 The designed sample of the adaptive fuzzy-neural model is shown in Fig. 5.

270

271 2.3.5. All subset regression method

272 In this study, after determining the map of suitable areas and preparing land suitability classes for
 273 ARG, the correlation between all parameters with these classes in 50 sampling points is calculated
 274 using Pearson regression. In most studies, stepwise regression is used to determine the relationship
 275 between all the effective factors separately (Rencher and Pun, 1980). In this study, the best subset
 276 regression is used to solve this problem. This regression model considers the combined effects of

277 all factors and provides more information about the combination of all factors while being reliable
278 (Anthony, 1984).

279

280 **3. Results and Discussion**

281 *3.1. Fuzzy method*

282 The fuzzy maps prepared for effective parameters in the ARG are shown in Fig. 6 for the input
283 parameters of Fig. 3. The membership function value for each parameter is between 0 and 1 which
284 represent less and more suitable locations for ARG, respectively.

285 As can be seen in Fig. 6, it is clear that small parts of the north of the region with high altitudes,
286 parts of the north and south of the region with low slope, most areas with less distance from the
287 fault, areas with land use of rangeland, areas prone to erosion, areas with high precipitation in the
288 northern parts, and areas with high drainage density located in the northern and southern parts of
289 the region are prone to ARG and receive the number 1 and cole 1 from the membership function.

290 Finally, to prepare a land suitability map for ARG using the pairwise comparison matrix, the
291 weighted fuzzy maps of input parameters are prepared (Fig. 7). According to the results, the slope
292 and elevation with the weight of 0.297 and 0.045 are of high and low importance, respectively.

293 It is worth noting that the weighting is done based on the conditions of the region and the opinions
294 of experts. The values of these weights can be different in different regions. For example, in the
295 studies of Rajasekhar et al. (2019), the lowest weight was considered for soil and lineament density
296 while in the study of Anand et al. (2020) the highest weight was considered for the lineament
297 parameter.

298 Finally, using the weights assigned to each parameter (Fig. 7), the final map of suitable areas for
299 ARG is prepared which is shown in Fig. 8. According to Fig. 8, it is obvious that about 12% of the

300 area is in the very high class (0.8-1), 14% in the high class (0.6-0.8), 59% in the moderate class
301 (0.6-0.4), 14% in the low class (0.2-0.4) and about 1% in the very low (0-0.1) class.

302

303 3.2. OWA-AHP method

304 In the present study, six order weights (α values) are used for seven factors that are rank-ordered
305 for each parameter. Based on the corresponding criterion weights and the standardized criterion
306 maps, OWA operators are defined. According to Table 3, α values is from at least one ($\alpha = 0$) to
307 all ($\alpha = \infty$) (Table 3).

308 Fig. 9 shows six alternatives of ARG with different risk levels. Fig. 9 (LLRNTO) and (LLRATO)
309 represent a low risk with the average tradeoff in comparison to Fig. 9 (ALRFTO) with more risk.
310 Fig. 9 (HLRATO) displays high risk with average tradeoff compared to Fig. 9 (LLRNTO) with
311 lower risk. Finally, Fig. 9 (ALRNTO) displays average risk with no tradeoff versus Fig. 9 (6) with
312 more risk. Based on Fig. 9, with reducing risk (low level of risk and no tradeoff as shown in Fig.
313 9 (LLRNTO)), the percentage of suitable location is low and only small portions of the eastern
314 part of the study area are suitable for the artificial recharge. By increasing the risk (LLRATO)
315 (Fig. 9 (LLRATO)), the eastern part of the region (blue color) turns into suitable for artificial
316 recharge. With average risk (full tradeoff as shown in Fig. 9 (ALRFTO)), all of the effective
317 parameters of drinking water quality with different weights lead to the highest appropriateness in
318 the north, south, and west parts of the region. Fig. 9 (ALRNTO) shows an average level of risk
319 and no tradeoff and has low risk compared to Fig. 9 (HLRATO). According to Fig. 9 (ALRNTO),
320 many parts of the study area have high values by a total rate of 28% (dark blue), medium value,
321 and a low value. According to Fig. 9 (HLRNTO), with a high level of risk and no tradeoff, the area
322 with appropriateness for ARG increases. So with decreasing the risk (no tradeoff), almost all parts

323 of the study area are found inappropriate for ARG. On the other hand, increasing the risk (no
324 tradeoff) leads to improvement in-inappropriateness for ARG.

325 According to Fig. 9, the area of land suitability maps with different risk levels is classified in
326 eighty classes shown in Fig. 10. For situations, LLR-NTO, LLR-ATO, ALR-FTO, classes 0-0.125
327 have the most area and for situations, ALR-NTO, HLR-ATO, HLR-NTO, classes 0.625-0.75, and
328 0.75-0.875 have the most area. Also, based on Fig. 10, land suitability with LLR-NTO had the
329 highest area in the very low class (80%) (between 0.125 - 0.25) while land suitability with HLR-
330 NTO had the highest area in the very high class (27%) (between 0.75 - 0.875).

331 This study applied OWA operators to prepare different maps with different risk levels for ARG.
332 Based on the financial and environmental situations, decision-makers can choose one of the maps
333 to manage the region. A review of the literature shows that there is no study about preparing an
334 ARG map with different risk levels using the OWA-AHP method. In the past, OWA has been used
335 in environmental engineering studies to investigate different parameters such as flood analysis
336 (Yalcin et al., 2004), environmental monitoring (Stroppiana et al., 2009), climate change
337 (Zarghami and Rahmani, 2012), soil fertility (Mokarram and Hojati et al., 2017), land suitability
338 (Mokarram and Aminzadeh, 2010).

339 Finally, to evaluate the accuracy of the two methods (fuzzy-AHP and OWA-AHP with ALR-NTO)
340 in 20 sample points, the values of climatic, human, environmental, topographic characteristics as
341 well as land suitability classes predicted by the two methods and the real values are compared
342 using the receiver operating characteristic (ROC) curve, the results of which are shown in Table
343 4. According to Table 4, it is clear that the area under curve (AUC) values for both models are
344 high (AUC Fuzzy-AHP = 95.0%, AUC OWA = 90.0%), which indicates the high accuracy of the
345 methods to determine suitable locations for artificial recharge of groundwater.

346 The results of the present study show that the AHP and OWA methods have high accuracy for
347 investigating suitable areas for groundwater recharge. The results of the study of Anand et al.
348 (2020) showed that the use of MCDA and GIS methods is an efficient and useful tool for planning
349 and improving areas suitable for groundwater recharge in the case area.

350

351 3.3. ANFIS method

352 Grid, sub-clustering, and FCM models from the ANFIS algorithm are used to predict land
353 suitability classes. For the three models, hybrid and back-propagation modes are used. Table 5 and
354 Fig. 11 show the results of each model. The results of FCM in hybrid mode to predict suitable
355 locations for ARG classes are shown in Fig. (11 (a)). R, MSE, and RMSE values are used to
356 determine the accuracy of the model in predicting land suitability classes. The results show that R
357 $= 0.99$, $MSE = 0$, $RMSE = 0.012$, indicating the high accuracy of the FCM model in hybrid mode
358 to predict suitable places for arterial recharge of groundwater. According to Fig. 11 (b), it is clear
359 that the sub-clustering method with values of $R = 1$, $MSE = 0$, and $RMSE = 0$ is highly accurate
360 in predicting land suitability classes. It is worth noting that the back-propagation model has more
361 errors and is not suitable for predicting land suitability classes. . Jafari et al. (2021) showed that
362 the FCM-hybrid method show high accuracy for checking groundwater status.

363 Studies show that the combination of the FCM method with hybrid mode for classification and
364 prediction of the target shows high accuracy, which is consistent with the results of this study
365 (Jaypuria et al., 2020; Jafari et al., 2021).

366 Then, to investigate the effective parameters on suitable places for ARG and to determine the most
367 important effective parameters, the best subset regression is used. Fan et al. (2020) confirmed the
368 high accuracy of the method in selecting the important data. According to Fig. 12, in the lowest

369 C_p values (5.2), slope, lithology, land use, altitude have the highest correlation and, therefore, have
370 the greatest impact on determining suitable locations for ARG.
371 Therefore, the use of the best subset regression method has a high accuracy due to the investigation
372 and selection of the most important parameters considering the combined relationship of the
373 parameters with each other (Takano and Miyashiro et al., 2020; Kwong et al., 2020).

374

375 **4. Conclusion**

376 In this study, fuzzy AHP and OWA-AHP methods are used to determine suitable locations for
377 ARG in Bushehr province, southern Iran. The results of the OWA-AHP method show that, with
378 decreasing risk level (no trade-off), almost all of the study area (i.e. about 80% or 34296.98 Km²),
379 except for small parts in the center and north of the study area, is suitable for ARG. Also, with
380 increasing the risk (no trade-off), about 27% (11575.23 Km²) of the study area is suitable for ARG,
381 and that the majority of these sites are spread over different parts of the study area, especially in
382 the south of the study area. By referring to land suitability maps with different risk levels, one of
383 them can be chosen depending on the financial constraints and environmental situations to
384 determine high-risk areas in the region. Therefore, based on different conditions of the study area
385 such as the people's financial status, authoritative perspectives, short and long-term plans, the age
386 distribution of the population, etc., the artificial recharge map with the appropriate risk level can
387 be used for the management of the region. Also, the results of the ANFIS method show that FCM
388 and sub-clustering are highly accurate in predicting land suitability map for ARG. Finally, the
389 results of the best subset regression method show that the slope, lithology, land use, and altitude
390 are the most important parameters to predict land suitability classes. In this study, it is also
391 suggested that in areas that are suitable for groundwater recharge, the necessary management

392 should be taken to feed runoff in groundwater aquifers.

393

394 **Acknowledgments:** The author would acknowledge Shiraz University for their kind help. This
395 study is financially supported by Shiraz University (238726-135).

396

397 **Notes on contributors:** Conceptualization by M.M., S.N. and A.A.; formal analysis by M.M.;
398 initial methodology and investigation by M.M., S.N. and A.A.; project administration by A.A.;
399 supervision by M.M.; validation M.M., and A.A.; visualization and software by M.M.;
400 writing—original draft by and M.M. and A.A.

401

402 **Declaration of competing interest**

403 No known

404

405

406 **References**

407

408 Anand B, Karunanidhi D, Subramani T. 2020. Promoting artificial recharge to enhance
409 groundwater potential in the lower Bhavani River basin of South India using geospatial
410 techniques. *Environ. Sci. Pollut. Res. Int.* 387-396.

411 Arya S, Subramani T, Karunanidhi D. 2020. Delineation of groundwater potential zones and
412 recommendation of artificial recharge structures for augmentation of groundwater resources
413 in Vattamalaikarai Basin, South India. *Environ. Earth Sci*, 79(5), 1-13.

414 Arya S, Subramani T, Karunanidhi D. 2020. Delineation of groundwater potential zones and
415 recommendation of artificial recharge structures for augmentation of groundwater resources
416 in Vattamalaikarai Basin, South India. *Environ. Earth Sci*, 79(5), 1-13

417 Ban AI, Ban OI. 2012. Optimization and extensions of a fuzzy multicriteria decision making
418 method and applications to selection of touristic destinations. *Expert Syst. Appl*, 39(8), 7216–
419 7225.

420 Bellmann RE, Zadeh LA. 1970. Decision making in a fuzzy environment *Management*
421 *Science* 2970. Bd.

422 Chu TC, Lin YC. 2009. An interval arithmetic based fuzzy TOPSIS model. *Expert Syst. Appl*,
423 36(8) 20870–10876.

424 Das B, Pal SC. 2019. Combination of GIS and fuzzy-AHP for delineating artificial recharge
425 of ground waterpotential zones in the critical Goghat-II block of West Bengal,
426 India. *HydroResearch*, 2, 21-30.

427 Fan J, Guo Y, Zhu Z. 2020. When is best subset selection the "best"?. *arXiv preprint*
428 *arXiv:2007.01478*

429 FAO. 2017. Water for Sustainable Food and Agriculture A report produced for the G20
430 Presidency of Germany. Retrieved from www.fao.org/publications
431 Ghayoumian J, Saravi MM, Feiznia S, Nouri B, Malekian A. 2007. Application of GIS
432 techniques to determine areas most suitable for artificial groundwater recharge in a coastal
433 aquifer in southern Iran. *J. Asian Earth Sci.*, 30(2), pp.364-374
434 Jafari MM, Ojaghlou H, Zare M, Schumann GJP. 2021. Application of a Novel Hybrid
435 Wavelet-ANFIS/Fuzzy C-Means Clustering Model to Predict Groundwater
436 Fluctuations. *Atmosphere*, 12(1), 9
437 Jaypuria S, Mahapatra TR, Tripathy S, Nakhale S, Gupta SK. 2020. Fuzzy C-means
438 Clustering-Based ANFIS Regression Modeling of Hybrid Laser-TIG Fabrication. *J. Achiev.*
439 *Mater. Manuf. Eng.* (pp. 617-624). Springer, Singapore
440 Kamangar M, Katorani S, Tekyehhah J, Sohrabneja C, Haderi FG. 2019. A novel hybrid
441 MCDM model select a suitable location for implement groundwater recharge. *Plant*
442 *Arch.*, 19(2), pp.87-98
443 Karunanidhi D, Aravinthasamy P, Sub ramani T, Roy PD, Srinivasamoorthy K. 2019. Risk of
444 fluoride-rich groundwater on human health: remediation through managed aquifer recharge in
445 a hard rock terrain. *South India Nat Resour Res.*
446 Kim D. 1998. Improving the fuzzy system performance by fuzzy system ensemble. *Fuzzy*
447 *Sets and Systems*, 98(1), pp.43-56
448 Kim GB, Choi MR, Seo MH. 2018. Site selection method by AHP-based artificial neural
449 network model for groundwater artificial recharge. *J. Eng. Geol.*, 28(4), 741-753
450 Kwong YD, Mehta KM, Miaskowski C, Zhuo H, Yee K, Jauregu, A, Liu, KD. 2020. Using
451 best subset regression to identify clinical characteristics and biomarkers associated with

452 sepsis-associated acute kidney injury. *Am. J. Physiol. Renal. Physiol.*, 319(6), F979-F98

453 Malczewski J, Chapman T, Flegel C, Walters D, Shrubsole D, Healy MA. 2003. GIS–
454 multicriteria evaluation with ordered weighted averaging (OWA): case study of developing
455 watershed management strategies. *Environ. Plan A*, 35(10), 1769-1784

456 Malczewski J, Rinner C. 2005. Exploring multicriteria decision strategies in GIS with
457 linguistic quantifiers: A case study of residential quality evaluation. *J. Geogr. Syst*, 7(2) 249–
458 268. <https://doi.org/10.1007/s10109-005-0159-2>.

459 Malczewski J. 2006. Ordered weighted averaging with fuzzy quantifiers: GIS-based
460 multicriteria evaluation for land-use suitability analysis. *Int. J. Appl. Earth Obs.*, 8 270–277.
461 <https://doi.org/10.1016/j.jag.2006.01.003>

462 McBratney AB, Odeh IOA. 1997. Application of fuzzy sets in soil science: Fuzzy logic, fuzzy
463 measurements and fuzzy decisions. In *Geoderma*, (77) 85–113. Elsevier.
464 [https://doi.org/10.1016/S0016-7061\(97\)00017-7](https://doi.org/10.1016/S0016-7061(97)00017-7)

465 Mokarram M, Aminzadeh F. 2010. GIS-based multicriteria land suitability evaluation using
466 ordered weight averaging with fuzzy quantifier: a case study in Shavur Plain, Iran. *ISPRS*,
467 38(2), 508–512.

468 Mokarram M, Hojati M. 2017. Using ordered weight averaging (OWA) aggregation for multi-
469 criteria soil fertility evaluation by GIS (case study: southeast Iran). *Comput. Electron.*
470 *Agric.*, (2017), 132, 1-13.

471 National Research Council. 1994. Ground water recharge using waters of impaired quality.
472 National Academies Press, <https://doi.org/10.17226/4780>

473 Palanisamy A, Karunanidhi D, Subramani T, Roy PD. 2020. Demarcation of groundwater
474 quality domains using GIS for best agricultural practices in the drought-prone Shanmuganadhi

475 River basin of South India. *Environ. Sci. Pollut. Res.* 387-398.

476 Patil KA, Khatik ND, Jirapure SN. 2020. Identification of Artificial Recharge Zones Using
477 GIS. In *International Conference on Emerging Trends in Engineering (ICETE)* (pp. 248-257).
478 Springer, Cham

479 Pazira A, Abdoli F, Ghanbari S. 2016. Moghdani, Comparison of fish species diversity in
480 Dalaki and Helleh Rivers of the Persis basin in Bushehr Province. *Iran J. Ichthyol.*, 3(3) 222–
481 228. <https://doi.org/10.22034/iji.v3i3.108>

482 Rajasekhar M, Raju GS, Sreenivasulu Y, Raju RS. 2019. Delineation of groundwater potential
483 zones in semi-arid region of Jilledubanderu river basin, Anantapur District, Andhra Pradesh,
484 India using fuzzy logic, AHP and integrated fuzzy-AHP approaches. *HydroResearch*, 2, 97-
485 108.

486 Rajasekhar M, Raju GS, Sreenivasulu Y, Raju RS. 2019. Delineation of groundwater potential
487 zones in semi-arid region of Jilledubanderu river basin, Anantapur District, Andhra Pradesh,
488 India using fuzzy logic, AHP and integrated fuzzy-AHP approaches. *HydroResearch*, 2,
489 pp.97-108

490 Rajasekhar M, Sudarsana Raju G, Imran Basha U, Siddi Raju R, Pradeep Kumar B,
491 Ramachandra M. 2019. Identification of Suitable Sites for Artificial Groundwater Recharge
492 Structures in Semi-arid region of Anantapur District: AHP Approach. *Hydrospatial*
493 *Analysis*, 3(1), 1-11

494 Rencher AC, Pun FC. 1980. Inflation of R² in best subset regression. *Technometrics*, 22(1),
495 pp.49-53

496 Saaty TL, Vargas LG. 1980. Hierarchical analysis of behavior in competition: Prediction in
497 chess. *Behav. sci.*, 25(3), pp.180-191

498 Stroppiana D, Boschetti M, Brivio PA, Carrara P, Bordogna G. 2009. A fuzzy anomaly
499 indicator for environmental monitoring at continental scale. *Ecol. Indic.*, 9(1), 92-106
500 Takano Y, Miyashiro R. 2020. Best subset selection via cross-validation criterion. *TOP*, 1-14
501 Wang YM, Parkan C. 2005. A minimax disparity approach for obtaining OWA operator
502 weights. *Inform. Sci.*, 175(1-2), pp.20-29
503 Yager RR. 1988. On ordered weighted averaging aggregation operators in multicriteria
504 decisionmaking. *IEEE T Syst Man Cy B*, 28(1) 283–190. <https://doi.org/10.1109/21.87068>
505 Yalcin G, Akyurek Z. 2004. Multiple criteria analysis for flood vulnerable areas. In *Proc. of*
506 *24th Annual ESRI International User Conference, San Diego, USA.*
507 Zarghami M, Rahmani MA. 2012. Aggregation of climate change predictions; Case study
508 from semi arid parts of Iran. In *IWA World Congress on Water, Climate and Energy, (2012),*
509 13-18.

510

Figure captions

511 **Fig. 1.** Flowchart of the research Method

512 **Fig. 2.** Location of the study area

513 **Fig. 3.** (a) Altitude (DEM); (b) Slope; (c) Distance to fault; (d) Land use; (e) Sensitivity classes;
514 (f) precipitation and (g) Drainage density maps

515 **Fig. 4.** Incremental and decrement membership function for each of the effective parameters in
516 groundwater recharge

517 **Fig. 5.** ANFIS structure

518 **Fig. 6.** Fuzzy maps for the ARG location parameters. (a) Altitude ; (b) Slope; (c) Distance to fault;
519 (d). Land use; (e). Lithology; (f). Precipitation; and (g) Drainage density

520 **Fig. 7.** Weights for used parameters using AHP

521 **Fig. 8.** Land suitable areas for ARG using the fuzzy-AHP method

522 **Fig. 9.** (1). LLR-NTO, (2). LLR-ATO, (3). ALR-FTO, (4). ALR-NTO, (5). HLR-ATO, (6). HLR-
523 NTO

524 **Fig. 10.** Area of each class using OWA method

525 **Fig. 11.** Results of ANFIS method. (a): Fcm:hybrid, (b): Sub:hybrid

526 **Fig. 12.** Best-subset regression results to determine the most important parameters affecting
527 artificial recharge of groundwater

528

Table 1. The data source of the study area to investigate suitable places for ARG

Parameters	Scale	Format	Source	Year
Slope	Resulation 30m	Raster	USGS	2019
Lithology	1:100,000	Polygon	Bushehr Geological Survey	2015
Land use	1:250,000	Polygon	Agricultural Jihad of Bushehr Province	2017
Drainage density	1:250,000	Raster	Geographical organization of the country	2015
Distance to fault	1:100,000	Polyline	Bushehr Geological Survey	2015
Precipitation	Resolution 30m	Raster	Bushehr Meteorological Organization	2019
Altitude	Resulation 30m	Raster	USGS	2019

529

530

531

Table 2. Description of sensitive classes of formation to water erosion

Classes	Description
1	Limestone rock
2	Bedded to massive fossiliferous limestone
3	Hale and chert, bedded to massive orbitolina limestone
4	Bedded argillaceous limestone and calcareous shale, bedded sandstone
5	Piedmont conglomerate and sandstone, shelly limestone
6	Bedded argillaceous - limestone, Low-level piedmont fan, and valley terrace deposits

532

Table 3. weighting each parameter with different α values (linguistic quantifiers)

j	Quantifier	Criterion Weight u^k	$(\sum_{k=1}^j u_k)^\alpha$	$(\sum_{k=1}^j u_k)^\alpha - (\sum_{k=1}^{j-1} u_k)^\alpha$
Slope		0.297	1	1
Lithology		0.231	1	0
Land use		0.167	1	0
Drainage density	(a) At least one, Low level of risk and no trade-off (LLR-NTO)	0.118	1	0
Distance to fault	($\alpha=0$)	0.082	1	0
Precipitation		0.059	1	0
Altitude		0.045	1	0
Slope		0.297	0.885678	0.885678
Lithology		0.231	0.938131	0.052453
Land use		0.167	0.96427	0.026139
Drainage density	(b) At least A Few, Low level of risk and average trade-off (LLR-ATO)	0.118	0.97951	0.015241
Distance to fault	($\alpha=0.1$)	0.082	0.988968	0.009458
Precipitation		0.059	0.995302	0.006334
Altitude		0.045	0.9999	0.004598
Slope		0.297	0.544977	0.544977
Lithology		0.231	0.726636	0.181659
Land use		0.167	0.833667	0.107031
Drainage density	(c) A Few, average level of risk and full trade-off (ALR-FTO)	0.118	0.901665	0.067999
Distance to fault	($\alpha=0.5$)	0.082	0.946044	0.044379
Precipitation		0.059	0.976729	0.030685
Altitude		0.045	0.9995	0.022771

Slope		0.297	0.297	0.142
Lithology		0.231	0.528	0.142
Land use		0.167	0.695	0.142
Drainage density	(d) Half, average level of risk and no trade-off (ALR-NTO)	0.118	0.813	0.142
Distance to fault	($\alpha=1$)	0.082	0.895	0.142
Precipitation		0.059	0.954	0.142
Altitude		0.045	1	0.142
Slope		0.297	0.088209	0.088209
Lithology		0.231	0.278784	0.190575
Land use		0.167	0.483025	0.204241
Drainage density	(e) Most, High level of risk and average trade-off (HLR-ATO)	0.118	0.660969	0.177944
Distance to fault	($\alpha=2$)	0.082	0.801025	0.140056
Precipitation		0.059	0.910116	0.109091
Altitude		0.045	0.998001	0.087885
Slope		0.297	0	0
Lithology		0.231	0	0
Land use		0.167	0	0
Drainage density	(g) All, High level of risk and no trade-off (HLR-NTO)	0.118	0	0
Distance to fault	($\alpha=\infty$)	0.082	0	0
Precipitation		0.059	0	0
Altitude		0.045	1	1

534

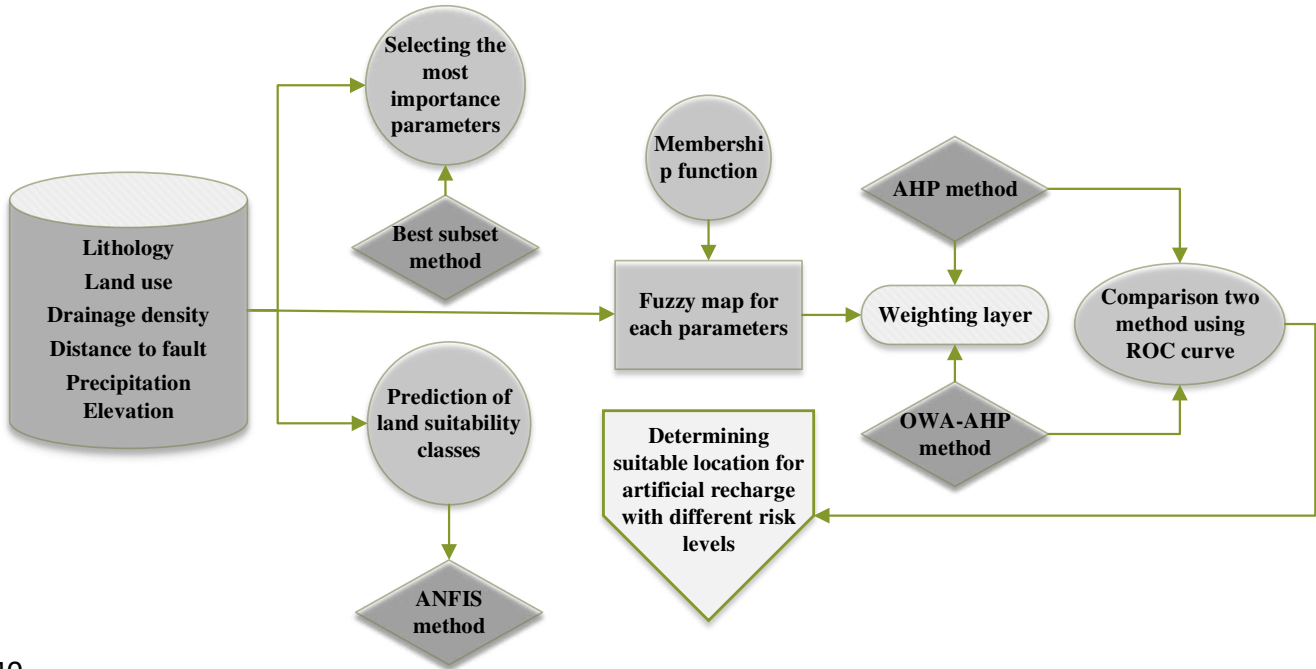
535

Table 4. Area Under the Curve of built models

Models	Area Under Curve (AUC)	Standard Error	Asymptotic Significant	Asymptotic 95%	
				Confidence Interval	
				Lower Bound	Upper Bound
Fuzzy- AHP	0.95	0.000	0.001	0.93	0.89
OWA	0.90	0.001	0.002	0.90	0.85

Table 5. The results of the ANFIS method

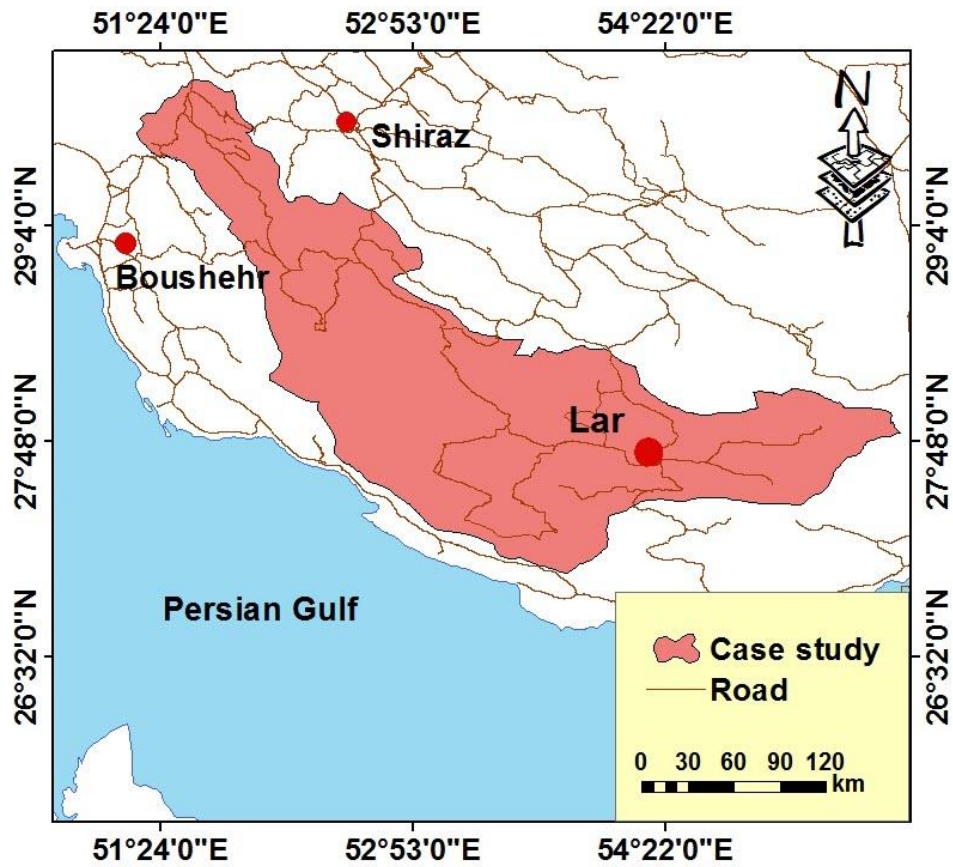
Method	Model	Train			Test		
		R	RMSE	MSE	R	RMSE	MSE
FCM	Back propagation	0.075	22.200	4.710	0.068	24.410	4.940
	Hybrid	0.990	0.000	0.012	0.990	0.000	0.012
Sub-cluster	Back propagation	0.430	44.230	6.650	0.570	28.400	5.300
	Hybrid	1.000	0.000	0.000	1.000	0.000	0.000
Grid-	Back propagation	0.560	0.730	0.270	0.730	10.370	3.220
	Hybrid	0.500	12.000	2.800	0.560	8.700	2.600



540

541

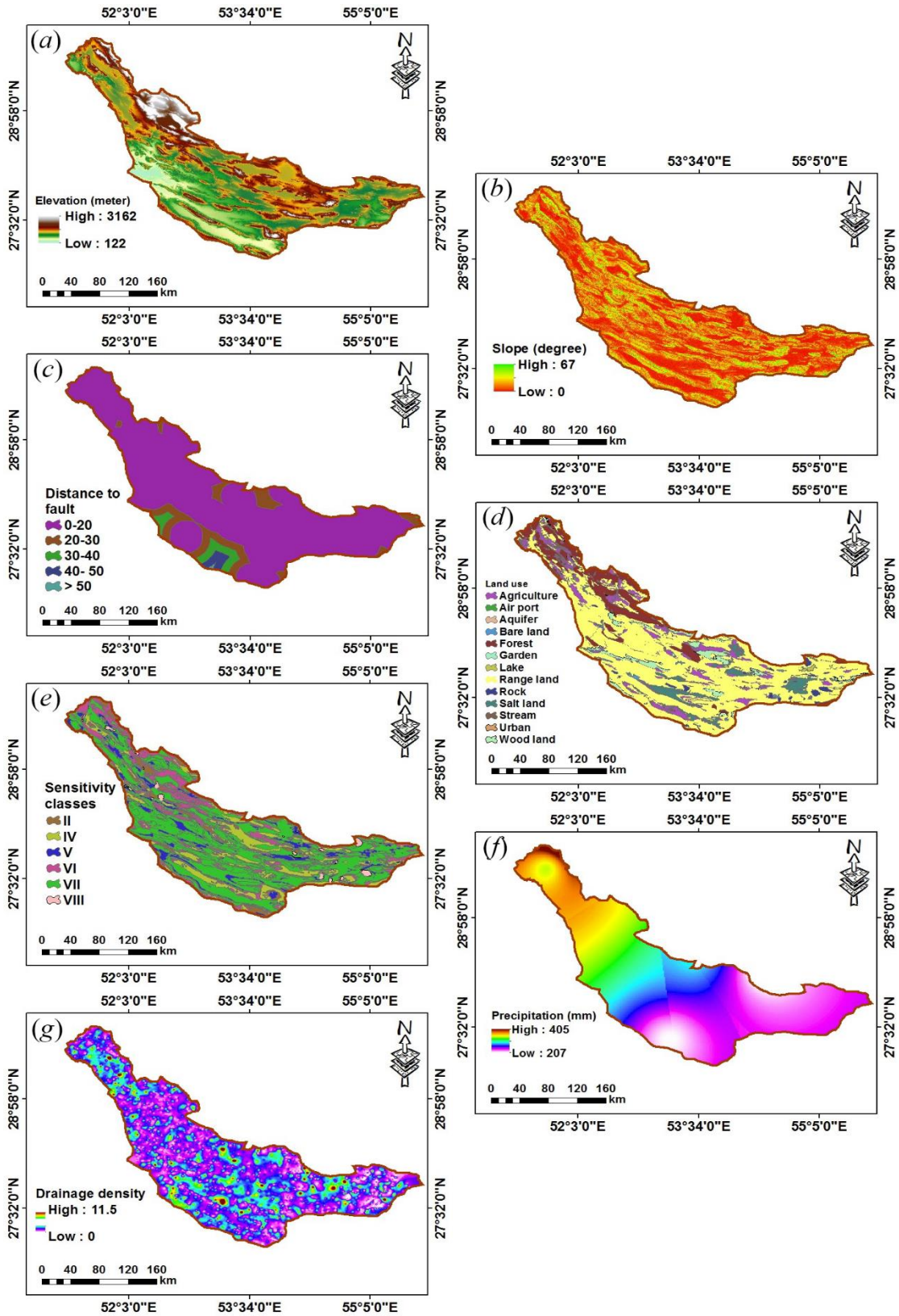
Fig. 1. Flowchart of the research Method



542

543

Fig. 2. Location of the study area



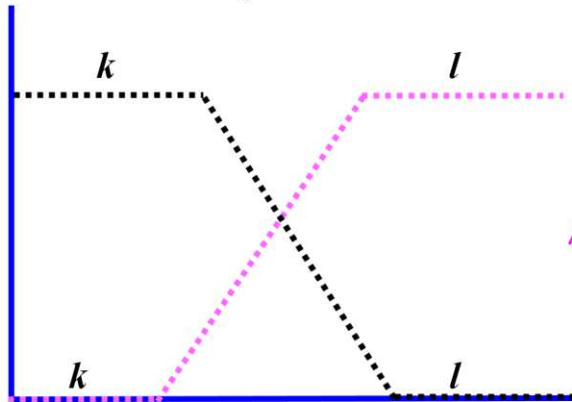
544

545 **Fig. 3.** (a) Altitude (DEM); (b) Slope; (c) Distance to fault; (d) Land use; (e) Sensitivity classes;

546

(f) precipitation and (g) Drainage density maps

$$\mu_A(x) = f(x) = \begin{cases} 0 & x \leq k \\ x - k / l - k & k < x < l \\ 1 & x \geq l \end{cases}$$



$$\mu_A(x) = f(x) = \begin{cases} 1 & x \leq k \\ l - x / l - k & k < x < l \\ 0 & x \geq l \end{cases}$$

547

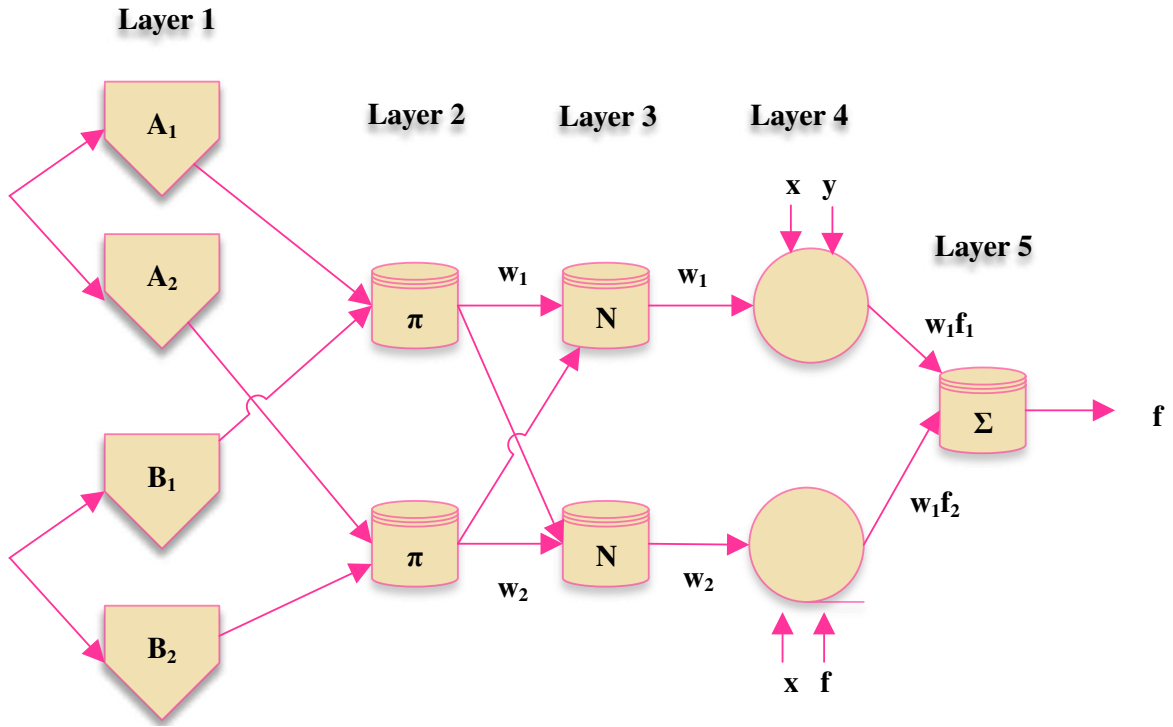
548 Fig. 4. Incremental and decrement membership function for each of the effective parameters in

549

groundwater recharge

550

551

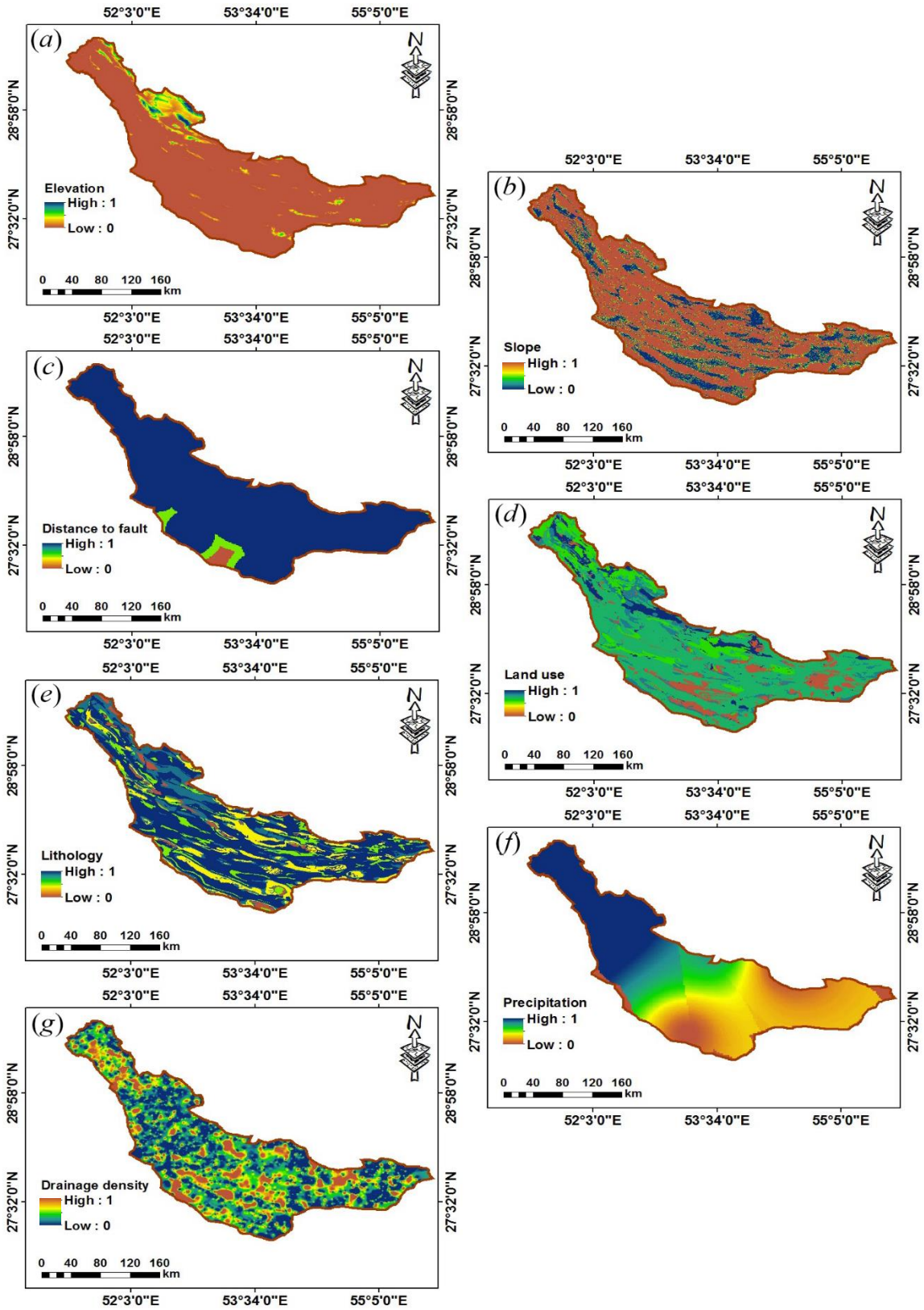


552

553

554

Fig. 5. ANFIS structure



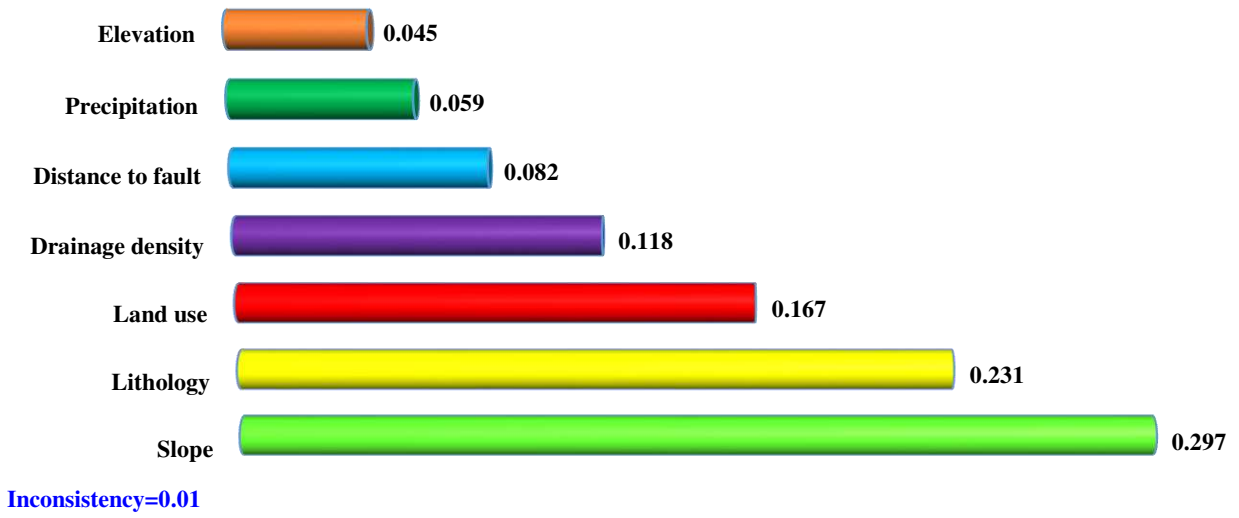
555

556

Fig. 6. Fuzzy maps for the ARG location parameters. (a) Altitude ; (b) Slope; (c) Distance to

557

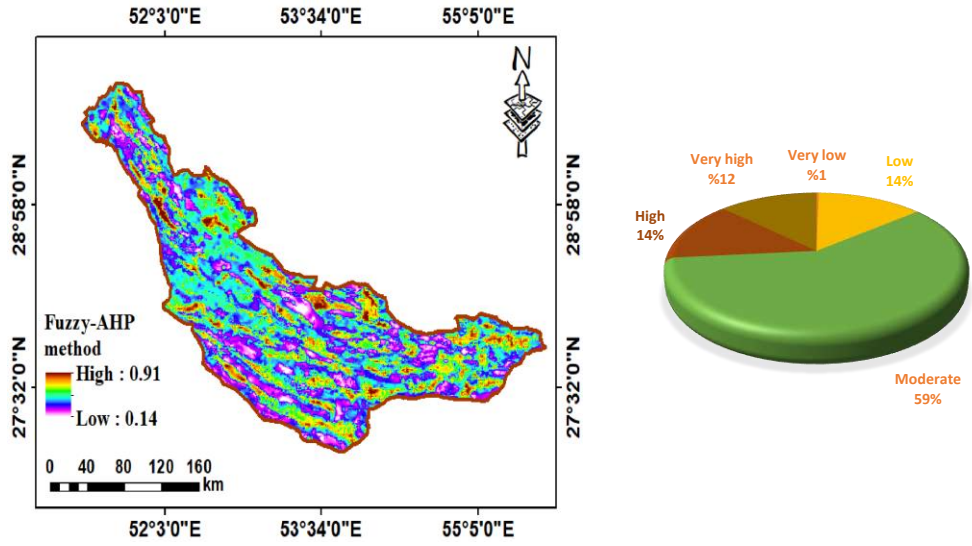
fault; (d). Land use; (e). Lithology; (f). Precipitation; and (g) Drainage density



558

559

Fig. 7. Weights for used parameters using AHP



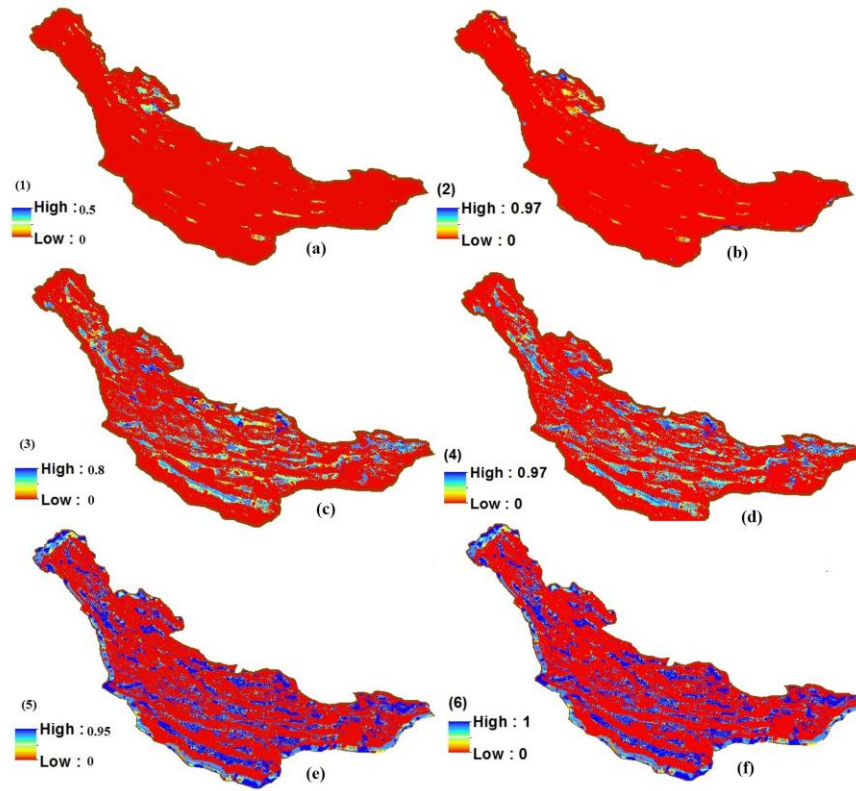
560

561

Fig. 8. Land suitable areas for ARG using the fuzzy-AHP method

562

563



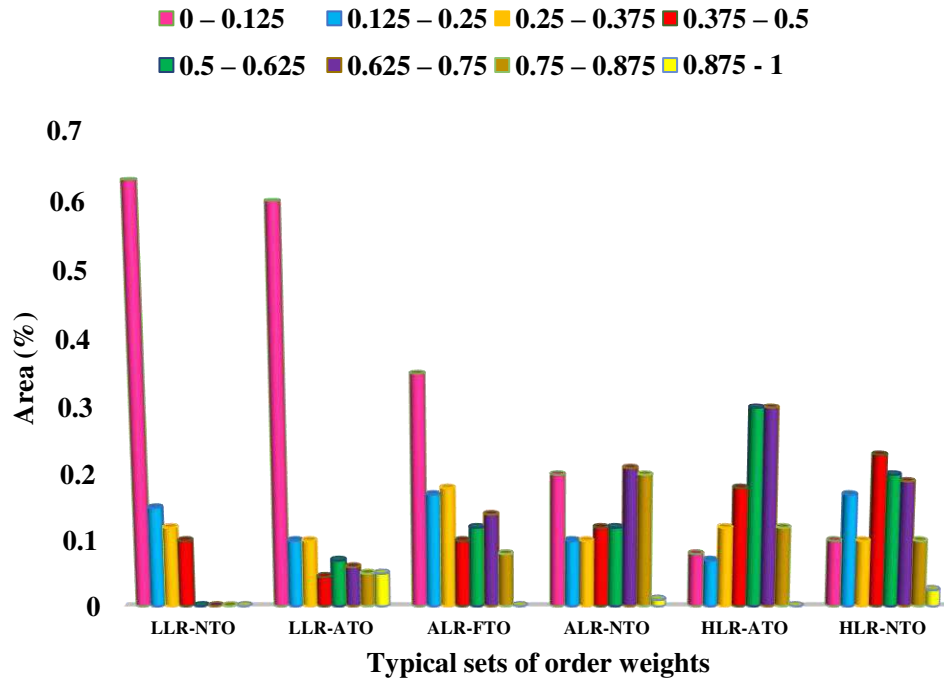
564

565

Fig. 9. (1). LLR-NTO, (2). LLR-ATO, (3). ALR-FTO, (4). ALR-NTO, (5). HLR-ATO, (6).

566

HLR-NTO



567

568

Fig. 10. Area of each class using OWA method

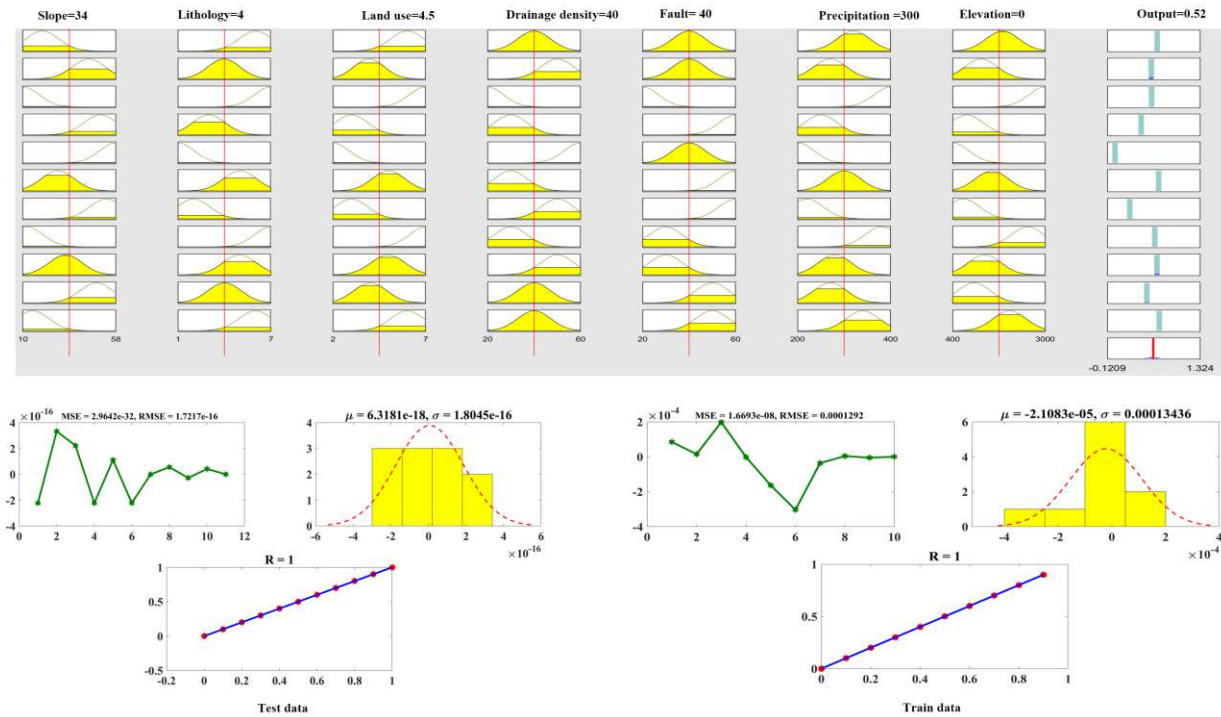
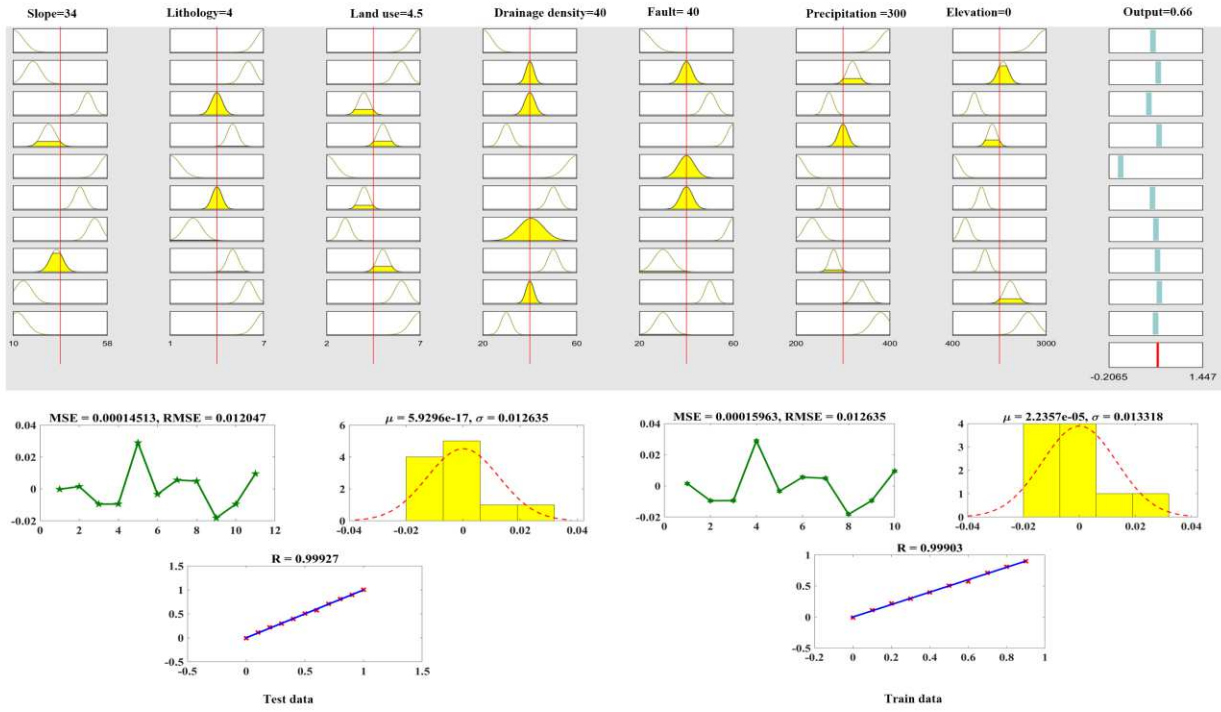


Fig. 11. Results of ANFIS method. (a): Fcm:hybrid, (b): Sub:hybrid

R ²	R ² _{adj}		C _p
97.6	97.3	Slope	13
97.6	97.3	Land use	12
99.3	99.1	Slope, Precipitation	9.7
98.9	98.6	Slope, Altitude	14.1
99.6	99.4	Slope, Lithology	5.7
99.5	99.3	Slope, Land use, Distance to fault	7.6
99.7	99.5	Slope, Land use, Distance to fault, Altitude	5.2
99.6	99.3	Slope, Land use, Drainage density, Distance to fault	7.5
99.8	99.5	Slope, Land use, Distance to fault, Precipitation	5.9
99.7	99.4	Slope, Land use, Distance to fault, Altitude, Precipitation	6.9
99.9	99.6	Slope, Land use, Distance to fault, Altitude, Precipitation, Lithology	6.1
99.8	99.4	Slope, Land use, Distance to fault, Precipitation, Lithology, Drainage density	7.9
99.9	99.5	Slope, Land use, Distance to fault, Precipitation, Lithology, Drainage density, Altitude	8

574

575

576

577

578

579

Fig. 12. Best-subset regression results to determine the most important parameters affecting artificial recharge of groundwater

Figures

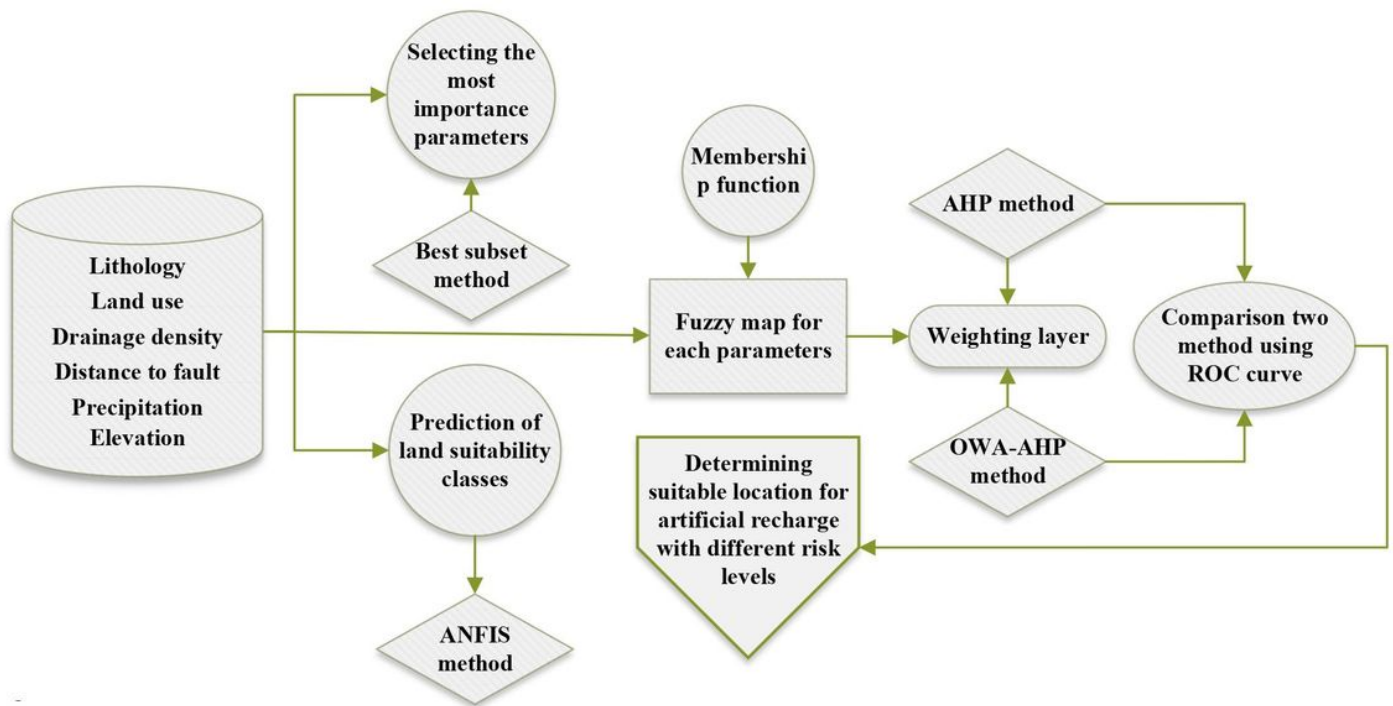


Figure 1

Flowchart of the research Method

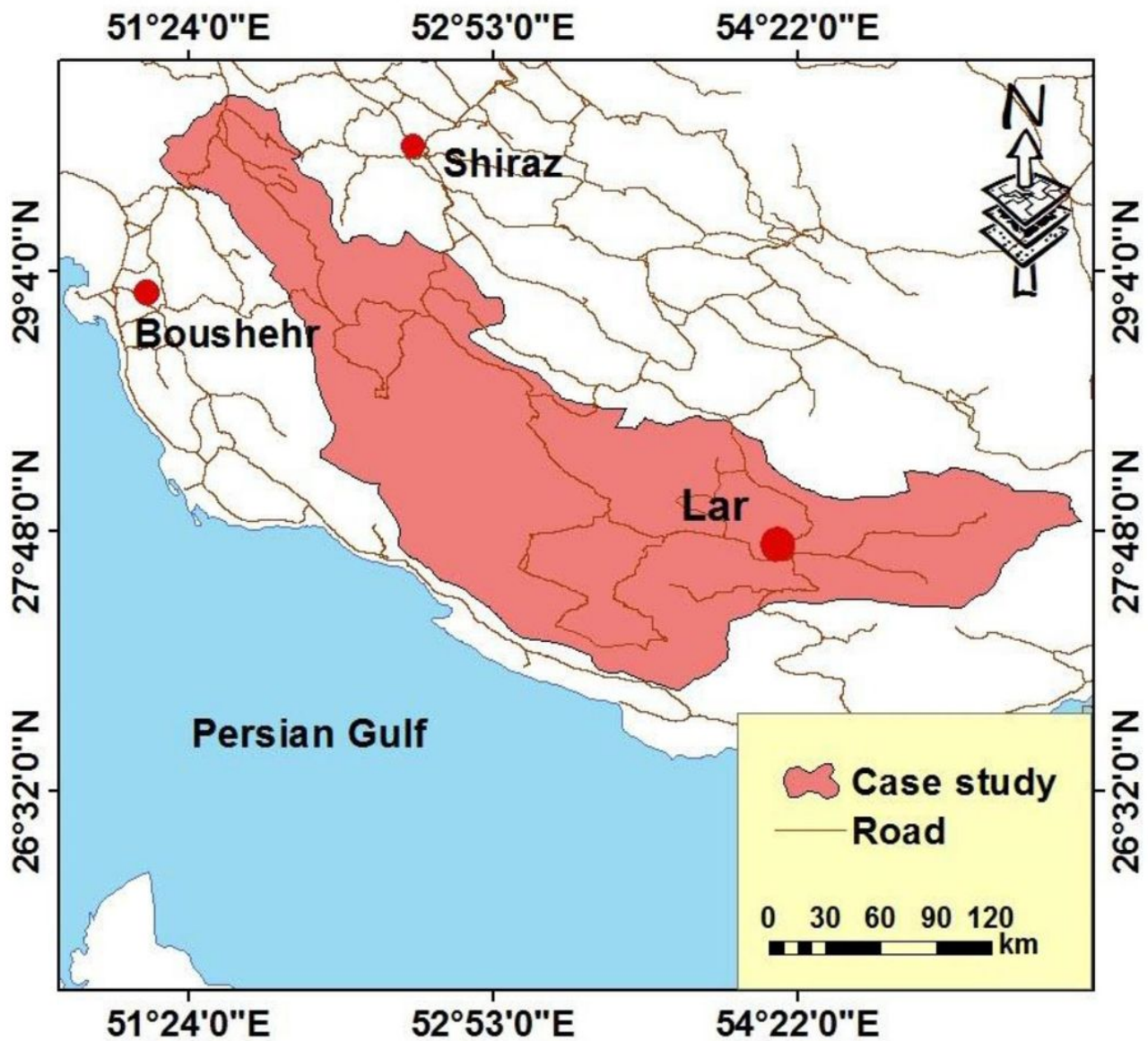


Figure 2

Location of the study area Note: The designations employed and the presentation of the material on this map do not imply the expression of any opinion whatsoever on the part of Research Square concerning the legal status of any country, territory, city or area or of its authorities, or concerning the delimitation of its frontiers or boundaries. This map has been provided by the authors.

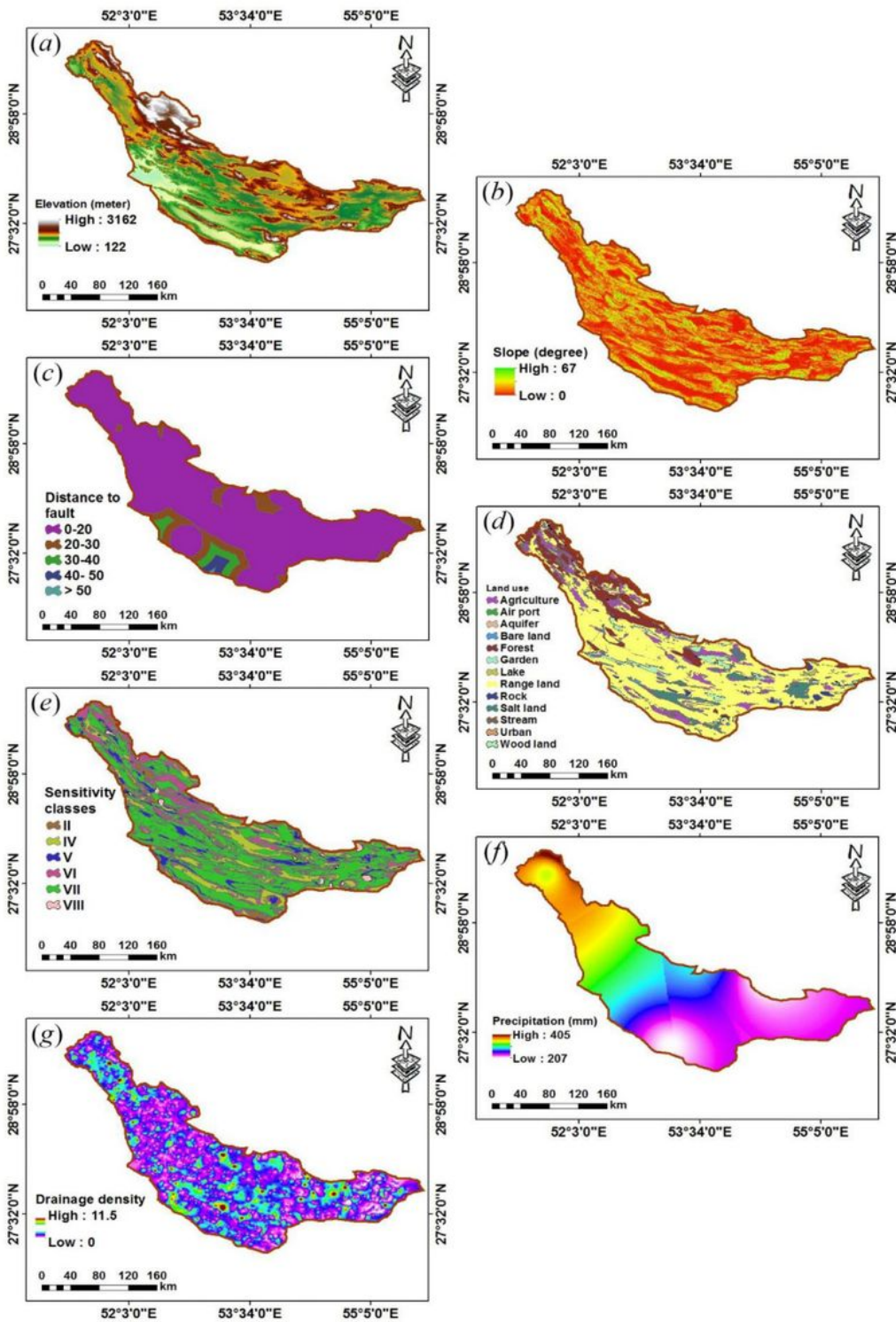


Figure 3

(a) Altitude (DEM); (b) Slope; (c) Distance to fault; (d) Land use; (e) Sensitivity classes; (f) precipitation and (g) Drainage density maps Note: The designations employed and the presentation of the material on this map do not imply the expression of any opinion whatsoever on the part of Research Square concerning the legal status of any country, territory, city or area or of its authorities, or concerning the delimitation of its frontiers or boundaries. This map has been provided by the authors.

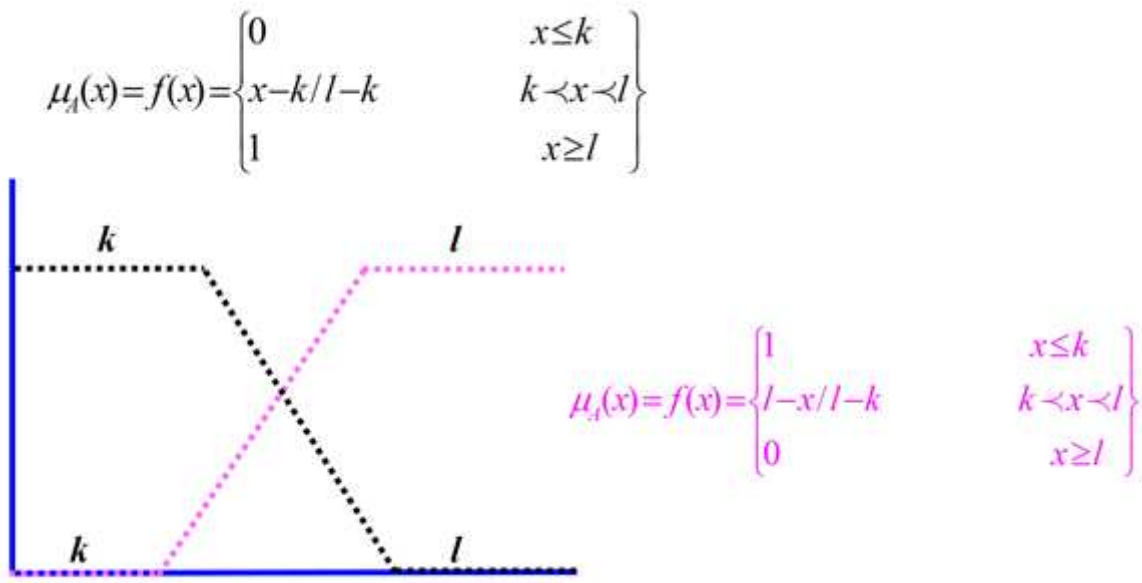


Figure 4

Incremental and decrement membership function for each of the effective parameters in groundwater recharge

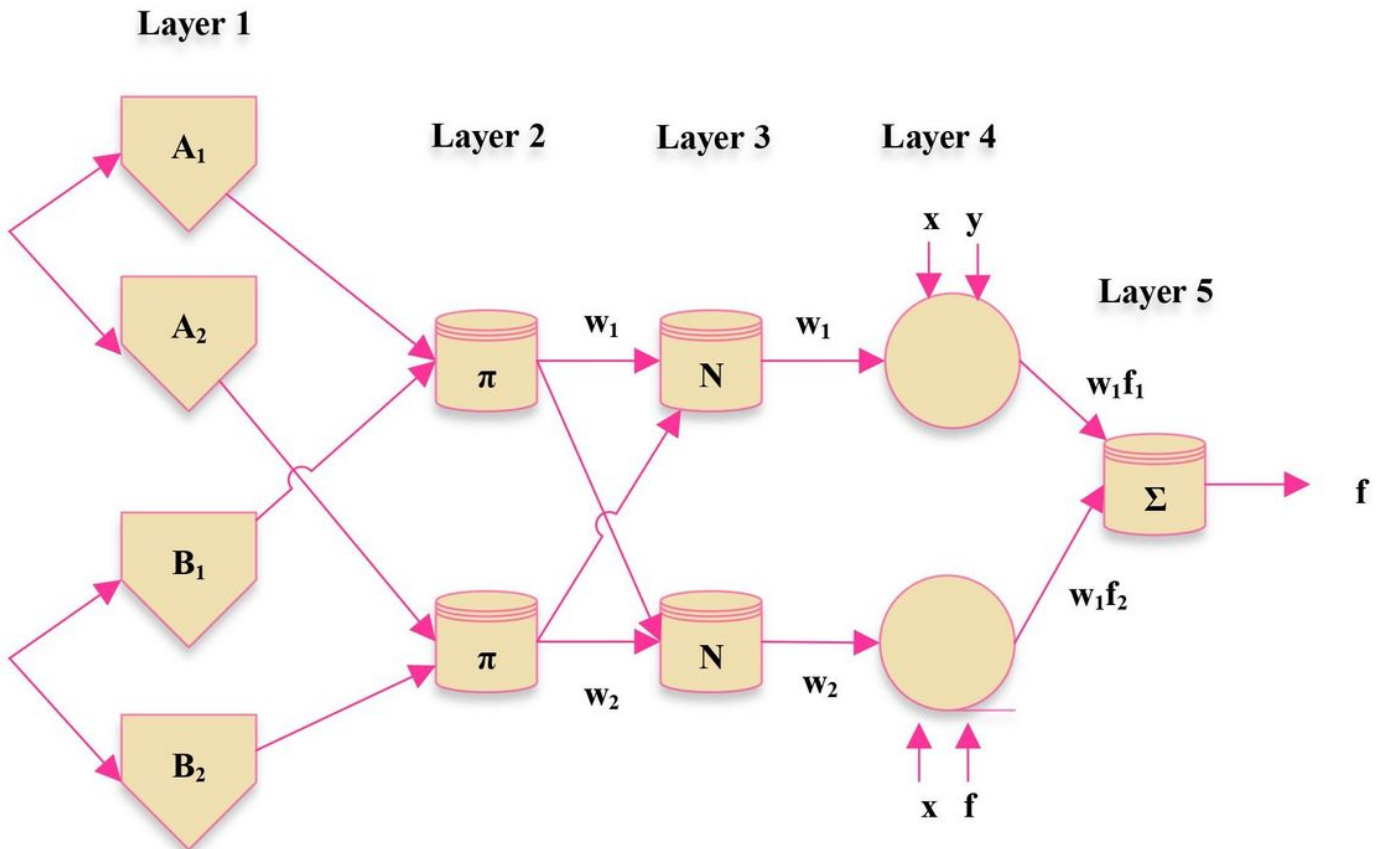


Figure 5

ANFIS structure

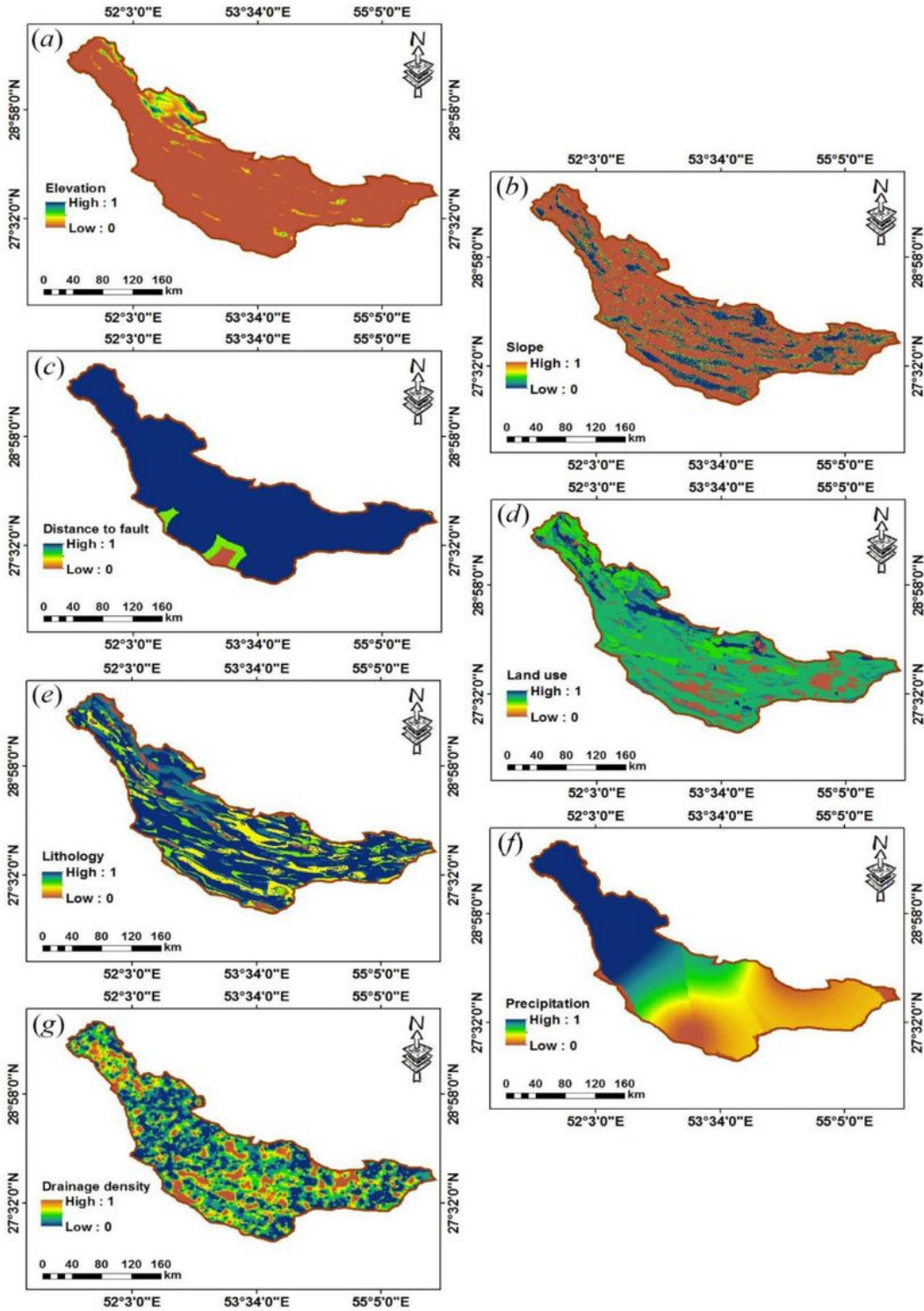


Figure 6

Fuzzy maps for the ARG location parameters. (a) Altitude ; (b) Slope; (c) Distance to fault; (d). Land use; (e). Lithology; (f). Precipitation; and (g) Drainage density Note: The designations employed and the

presentation of the material on this map do not imply the expression of any opinion whatsoever on the part of Research Square concerning the legal status of any country, territory, city or area or of its authorities, or concerning the delimitation of its frontiers or boundaries. This map has been provided by the authors.

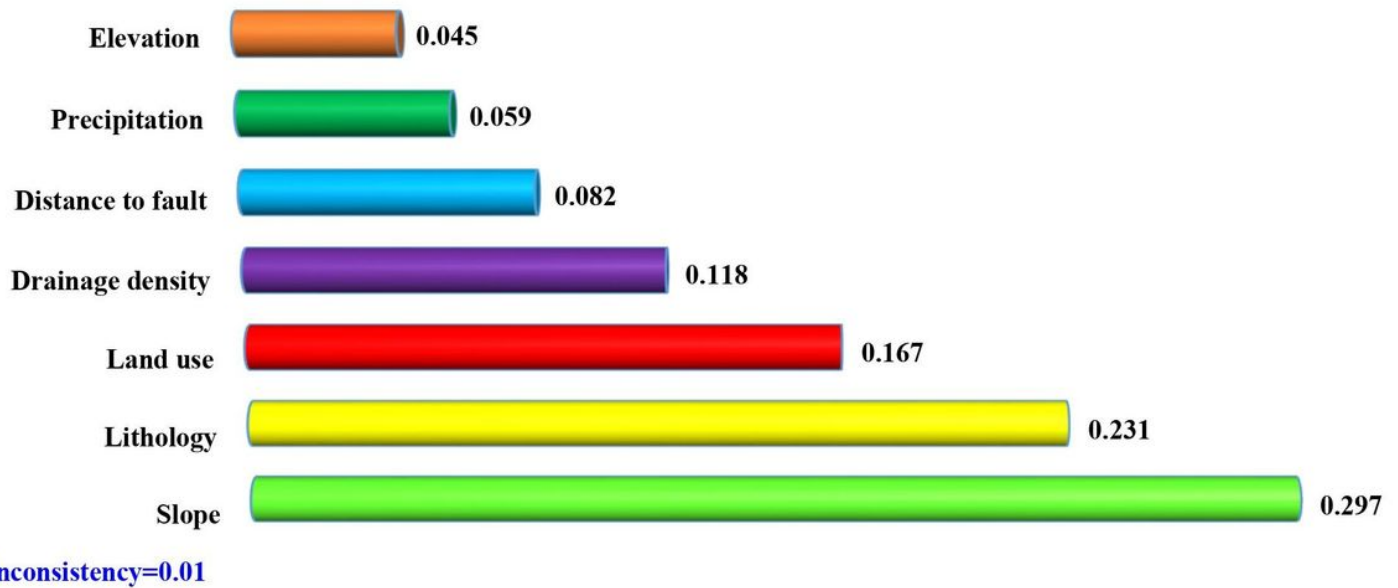


Figure 7

Weights for used parameters using AHP

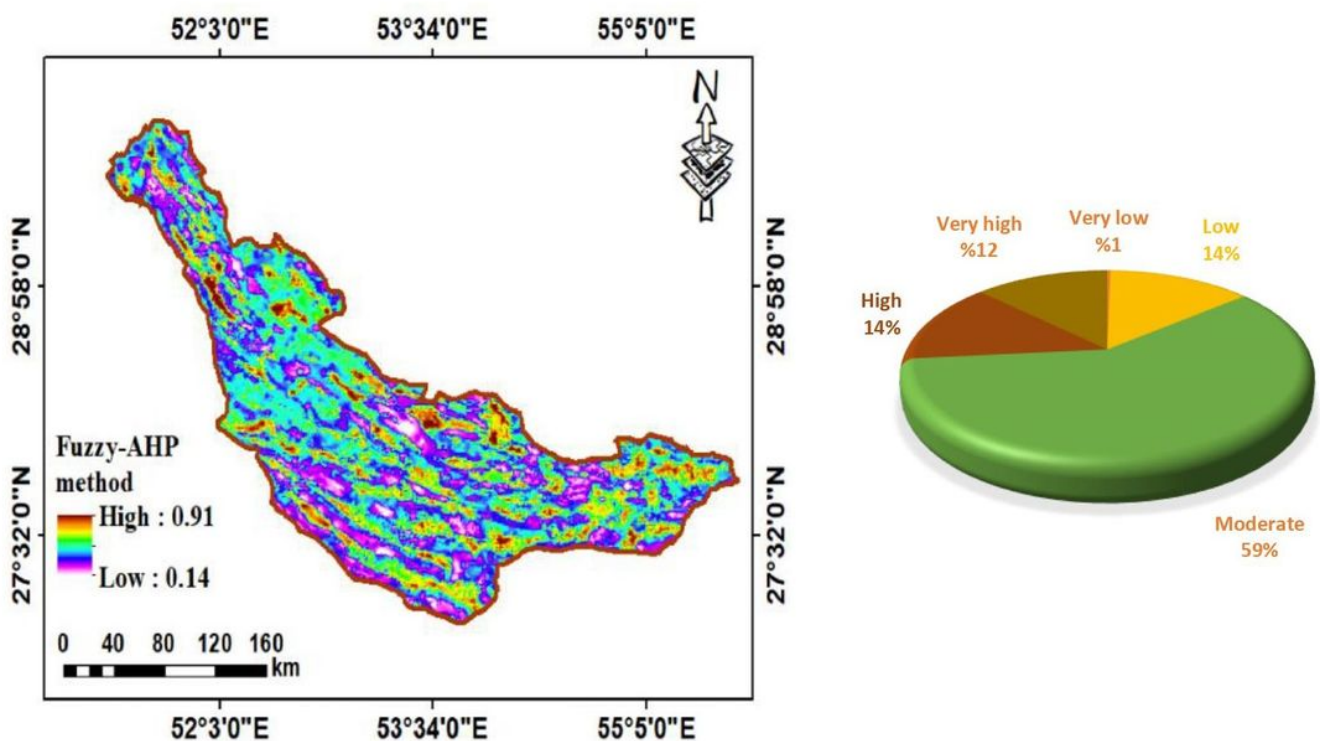


Figure 8

Land suitable areas for ARG using the fuzzy-AHP method Note: The designations employed and the presentation of the material on this map do not imply the expression of any opinion whatsoever on the part of Research Square concerning the legal status of any country, territory, city or area or of its authorities, or concerning the delimitation of its frontiers or boundaries. This map has been provided by the authors.

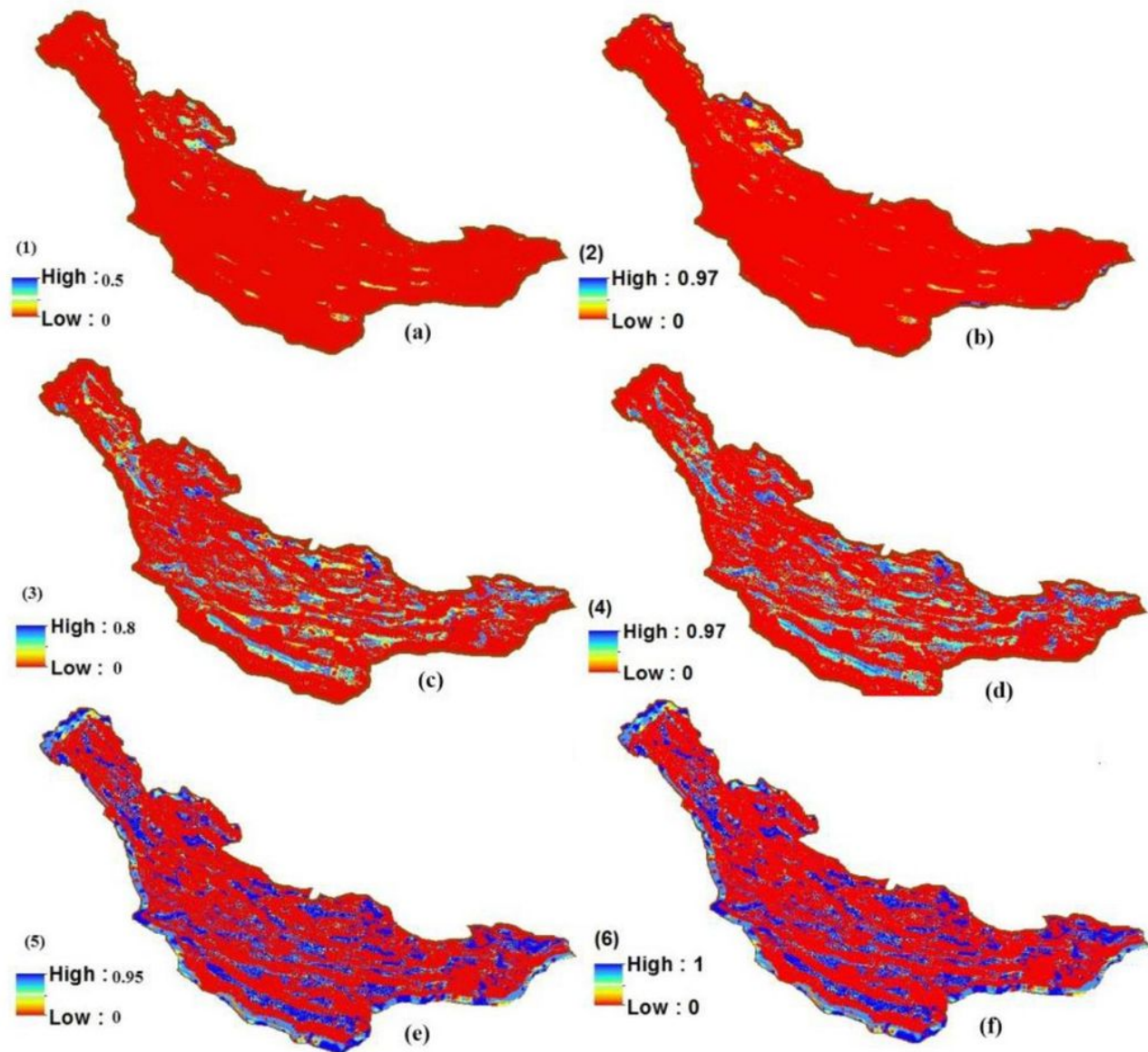


Figure 9

(1). LLR-NTO, (2). LLR-ATO, (3). ALR-FTO, (4). ALR-NTO, (5). HLR-ATO, (6). HLR-NTO Note: The designations employed and the presentation of the material on this map do not imply the expression of any opinion whatsoever on the part of Research Square concerning the legal status of any country,

territory, city or area or of its authorities, or concerning the delimitation of its frontiers or boundaries. This map has been provided by the authors.

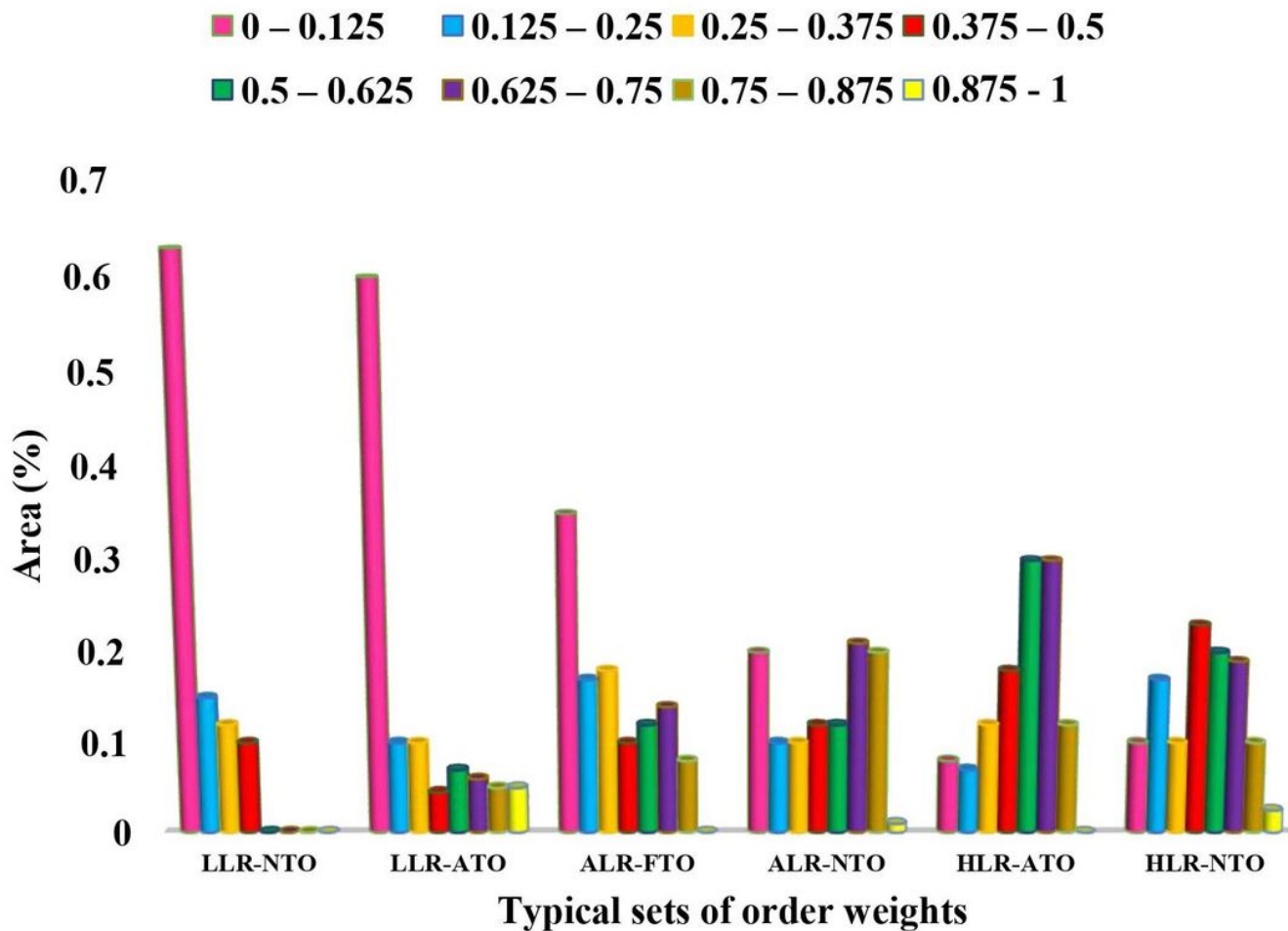


Figure 10

Area of each class using OWA method

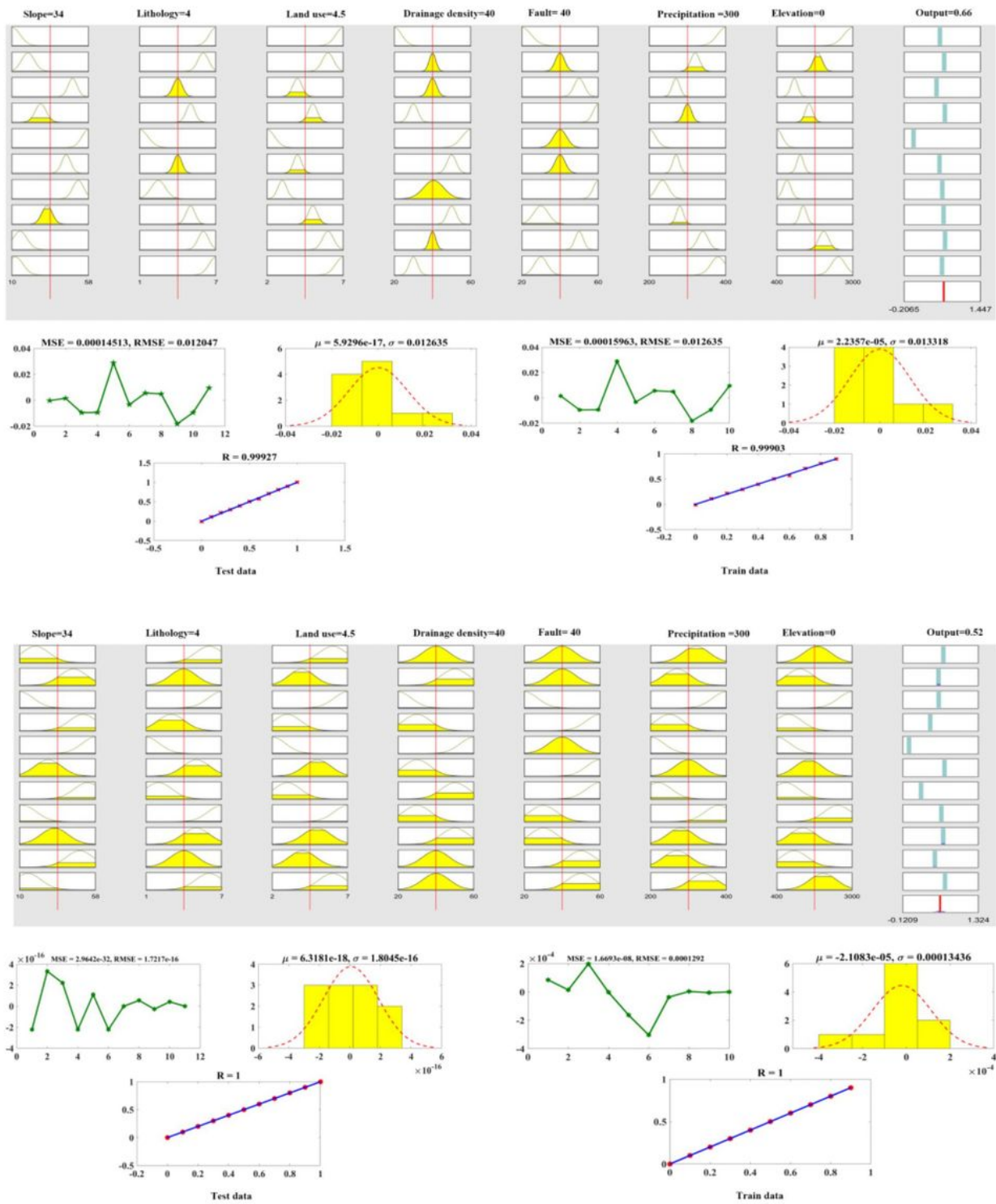


Figure 11

Results of ANFIS method. (a): Fcm:hybrid, (b): Sub:hybrid

R^2	R^{2adj}								C_p
97.6	97.3	█							13
97.6	97.3	█		█					12
99.3	99.1	█	█			█	█		9.7
98.9	98.6	█	█		█	█	█	14.1	
99.6	99.4	█	█		█	█		5.7	
99.5	99.3	█	█		█	█		7.6	
99.7	99.5	█	█		█	█		5.2	
99.6	99.3	█	█		█	█		7.5	
99.8	99.5	█	█		█	█		5.9	
99.7	99.4	█	█		█	█		6.9	
99.9	99.6	█	█		█	█		6.1	
99.8	99.4	█	█		█	█		7.9	
99.9	99.5	█	█		█	█		8	

Slope Lithology Land use Drainage density Distance to fault Precipitation Altitude

Figure 12

Best-subset regression results to determine the most important parameters affecting artificial recharge of groundwater